ANALYSIS OF DISSOLVED HEAVY METAL AND CESIUM ION REMOVAL USING MODIFIED HYDROGELS

A Thesis

by

SHANGBIN SUN

Submitted to the Office of Graduate and Professional Studies of
Texas A&M University
in partial fulfillment of the requirements for the degree of

MASTER OF SCIENCE

Chair of Committee,	Jenn-Tai Liang
Co-Chair of Committee,	Jerome J. Schubert
Committee Members,	Kung-Hui Chu
	Huili Guan
Head of Department,	A. Daniel Hill

May 2017

Major Subject: Petroleum Engineering

ABSTRACT

Oil and gas production, industrial manufacturing, mining, and agriculture all produce significant amounts of wastewater, often containing harmful heavy metal ions such as cadmium, lead, and arsenic. Radioactive disasters such as Chernobyl, Three Mile Island, and the Fukashima Daiichi nuclear accidents have introduced radioactive nuclides such as cesium-137 into water streams. These heavy metals and radionuclides, when ingested, can cause irreversible damage to human health. In this research, functionalized hydrogels with the ability to adsorb these contaminants have been synthesized. It is the purpose of this project to test and quantify how well these hydrogels can remove dissolved cadmium, lead, arsenic, and cesium.

The hydrogels for this research are PAAm (polyallylamine) modified with DHBA (2,3-dihydroxybenzoic acid), TGA (thioglycolic acid), and ferrocyanide. Tests with varying initial concentrations and contact times were performed for adsorption isotherm models, adsorption speeds, and kinetic models. Selectivity tests were performed to see how well the hydrogels dealt with competing contaminant species. Varying pH tests were performed to quantify how hydrogels handled different pH environments. Reusability tests were performed to see if and how many times these hydrogels can be reused. Finally, column studies were performed to see how well the hydrogels will perform in a steady state environment. All experimental samples were analyzed by an ICP-OES instrument.

Results from these experiments suggest that both the base PAAm and TGA modified heavy metal hydrogels have very high adsorption capacities, quick adsorption rates, and great reusability. The cesium capturing hydrogels also showed high adsorption capacities and quick adsorption rates, but was not able to be recovered using our methods. All three hydrogels showed adsorption capacities and rates which rival current research top performers and are promising for industry applications.

ACKNOWLEDGEMENTS

I would like to thank my committee chair, Dr. Liang, and my committee members, Dr. Schubert, Dr. Chu, and Dr. Guan, for their guidance and support throughout the course of this research, and Dr. Mohammadi for all of her contributions.

Thanks also go to my friends and colleagues and the department faculty and staff for making my time at Texas A&M University a great experience.

Finally, thanks to my mother, father, and sister for their encouragement.

CONTRIBUTORS AND FUNDING SOURCES

Contributors

This work was supervised by a thesis committee consisting of Professor Jenn-Tai Liang, and Professors Jerome Schubert and Huili Guan of the Department of Petroleum Engineering, and Professor Kung-Hui Chu of Civil Engineering.

The hydrogel synthesis was provided by Dr. Zahra Mohammadi. All other work conducted for the thesis was completed by the student independently.

Funding Sources

Graduate study was supported and funded by Dr. Jenn-Tai Liang from Texas A&M University Petroleum Engineering Department.

NOMENCLATURE

PAAm	Polyallylamine
DHBA	2,3-dihydroxybenzoic acid
TGA	Thioglycolic acid
ICP	Inductively coupled plasma
ICP-OES	Inductively coupled plasma optical emission spectrometry
MEUF	Micellar enhanced ultrafiltration
EDTA	Ethylenediamine tetraacetic acid
DPA	D-Penicillamine
DMSA	Meso-2,3-Dimercaptosuccinic acid
PB	Prussian blue
MBA	N,N'- methylenebisacrylamide
TEA	N,N,N -triethylamine
DMF	Dimethylformamide
DCC	Dicyclohexylcarbodiimide
NHS	N-hydroxysuccinimide
PT	PAAm/TGA
PTD	PAAm/TGA/DHBA

TABLE OF CONTENTS

Page

LIST OF FIGURES

Page

LIST OF TABLES

Page

1. INTRODUCTION

The objective of this research is to quantify the usefulness of functionalized adsorption hydrogels in the removal of dissolved cadmium, arsenic, lead, and cesium ions from water. Cadmium, lead, and arsenic are highly toxic pollutants that can be discharged from several different activities including production water, mining wastewater, and agricultural runoff [1-2], while radionuclides such as cesium isotopes can come from manmade nuclear incidents such as the Fukushima disaster in Japan. Increasing accumulation of heavy metals through the food chain can cause serious threats to human health like damaging the structure of DNA, nerves, livers, and bones [3], while cesium can induce medullar dystrophy, damage reproductive function, and cause liver disorders [4]. Many different methods for heavy metal removal have been implemented. These methods include chemical precipitation, solvent extraction, and adsorption. But these methods all have their drawbacks, including secondary pollution due to large amounts of organic solvents being used for solvent extraction [5] and the formation of toxic sludge after treatment for chemical precipitation [6]. For cesium removal, coagulation–sedimentation processes were analyzed to be effective in removing particle bound cesium but not soluble ions in water [7]. The method of contaminant removal in this research is adsorption onto hydrogels with multi-functionalized groups that chelate heavy metals and capture cesium. Hydrogels are soft materials with three-dimensional cross-linked networks that can contain up to 90% water. The high water content of these hydrogels is favorable for adsorption of foreign

ions. The hydrogel polyallylamine (PAAm), which was previously modified as a potential iron specific chelating agent, is the basic hydrogel used in this study [8]. This hydrogel is pH sensitive, containing amine groups that are natural chelators. For heavy metal adsorption, we introduced thioglycolic acid (TGA) and the phenolic group of dihydroxybenzoic acid (DHBA) onto PAAm. These additions contain thiol and hydroxyl groups meant to improve heavy metal chelation, selectivity, and affinity for our heavy metals by emulating metal intoxication antidotes used in the medical field [9]. Cesium removing hydrogels were inspired, on the other hand, by previous research using Prussian blue. Prussian blue is a chemical pigment crystal that contains several chemical groups called ferrocyanide. Ferrocyanide has cage-like structures formed from iron, carbon and nitrogen. Its cage size is similar to the hydration radius of cesium ions and could selectivity trap them from water. Problems with Prussian blue are its inability to be reused after adsorption and its powder form, making it hard to use for adsorption processes [10]. In this thesis, potassium ferrocyanide and sodium ferrocyanide were used as modifications onto PAAm to capture cesium. Our hypothesis is that by immobilizing the ferrocyanide group onto our hydrogel, it would be easier to use than the powder form and could still provide good cesium entrapment capacities.

Dr. Mohammadi provided all of the synthesized modified hydrogels according to her dissertation [20]. To accurately analyze the heavy metal and cesium samples, we used an inductively coupled plasma (ICP) instrument. Sorption experiments were conducted on the effects of pH, contact time, initial concentration of contaminants, selectivity, and recyclability. By analyzing the results based on time and initial

concentration, we were able to match our results with established models to better understand the mechanics of adsorption for our hydrogel. Finally, after all of the batch experiments, a column study was done on each of the hydrogels to determine how well they can perform in a steady state flow environment.

2. LITERATURE REVIEW

2.1 Heavy metal health concerns

The world health organization, a specialized agency part of the UN, dedicated a list of 10 chemicals of major public concern. These chemicals are all considered highly hazardous and detrimental to human and environmental health [11]. The three heavy metals we are concerned with in this research, cadmium, lead, and arsenic, are all on this list. Cadmium when inhaled can cause life threatening pulmonary problems, while ingested through food and water could cause major irreversible kidney damage. Long-term cadmium exposure could cause damage to the skeletal structure and increase risk of osteoporosis. Lead poisoning is a more well-known affliction that in acute cases can cause headaches, abdominal pains, and symptoms to the nervous system. Through long exposure, lead poisoning will cause brain damage, nerve damage, and kidney damage at levels higher than 100 µg/L in the bloodstream. Finally, arsenic, which is synonymous with poison in the English language, will cause gastrointestinal symptoms, severe disturbances of cardiovascular and central nervous systems, bone marrow depression, hemolysis, hepatomegaly, melanosis, polyneuropathy, and death. All three of these heavy metals are known to increase the risk of cancer [12].

Although the adverse health effects of these heavy metals have been known for a while, they can still be found discharged into waters from different industrial activities. Some parts of the world, especially less developed countries where environmental

regulations are traditionally more relaxed, are actually seeing a rise in heavy metal emissions and contamination.

The sources of these heavy metals can be numerous. Cadmium has been used as corrosion resistant plating on steel, PVC stabilizers, color pigments, and most commonly in re-chargeable batteries. Lead was commonly emitted from petroleum products in the last century before the introduction of unleaded petroleum and is still a contaminant from sources such as glass factories and mines. Finally, arsenic can be produced as a byproduct of smelting non-iron metals and burning fossil fuels. Production of arsenic pesticides and preservatives will also cause contamination of air and water [12]. All three of these heavy metals are present in petroleum production waters and various other manufacturing wastewaters, which can easily be sources of contamination for drinking water [1]. That is why in this research project we are focusing on the capture of dissolved heavy metals in water.

2.2 Radionuclide health concerns

With a half-life of 30+ years, radioactive isotope cesium-137 is considered one of the most problematic fission products known to mankind. In 1986, the city of Pripyat in the USSR saw the first level 7 event on the International nuclear event scale and is the worst nuclear power plant accident in history. The Chernobyl disaster released large amounts of radioactive particles into the atmosphere spreading to large parts of Europe. An estimated 400 times more radioactive material was released from this incident than the bombing of Hiroshima. Radioactive cesium-137 and cesium-134 were scattered and

dissolved in bodies of water such as the Pripyat River and the Dnieper reservoir system, which then were supplying water to 2.4 million people [13]. Then in 2011, 25 years after the Chernobyl disaster, Japan saw the second and currently only other level 7 nuclear disaster in the Fukushima Daiichi nuclear disaster. Following a string of earthquakes, a tsunami destroyed emergency generators used for cooling reactors causing three meltdowns and the release of radioactive isotopes including cesium-137 and cesium-134 [14]. On top of the nuclear disasters, other operations such as nuclear testing and everyday nuclear plant operations also produce cesium as a fission product. These radioisotopes have found their way to surface waters and ground waters polluting drinking and food sources and eventually climbing up the food chain to people.

The effects of cesium and other radioisotopes on animals and people have been well documented, with primary concerns of exposure being radiation sickness and increased risk of cancer. Radiation sickness, which is often caused by short exposure to high dosage of radiation, could cause nausea, vomiting, falling blood counts, and increased risk of infections [15]. While long exposure to cesium-137 means the body will be extensively exposed to carcinogenic high energy gamma radiation. An easy method for someone to be chronically exposed to radiation is internal exposure due to ingestion. Ingestion of radiative cesium allows for the material to be absorbed into muscle tissues, which would expose the surrounding body areas to harmful radiation even if this person was not living in a hot zone [17]. The simplest and most common way for this to happen is contamination of commonly used water sources. Radioactive cesium is able to form salts such as ^{137}CsCl that are soluble in water, which could then

easily enter the human body through drinking or eating of high radiation food previously exposed to the water. Since long term radiation exposure is most commonly from water sources, any effective cesium removal methods must include the ability to trap and remove cesium that has already dissolved.

2.3 Previous removal methods

Precipitation removal

Chemical precipitation removal is currently the most widely used process in industry for heavy metal removal. The processes are considered relatively simple to operate, and require chemicals to react with heavy metal ions to form insoluble precipitates. These precipitates are then separated by sedimentation and/or filtration. There are two main forms of chemical precipitation, hydroxide precipitation and sulfide precipitation.

Hydroxide precipitation is the usage of various hydroxide chemicals to precipitate metals from wastewaters. The pH for these environments are usually set to 8-10 to minimize solubility of the resulting precipitates [6]. The primary and most used chemical for this process is calcium hydroxide. Even though this process is widely used, there are some limitations. The small pH range for precipitation could cause problems during operations, while complexing agents are known to inhibit precipitation. Most importantly, the hydroxide precipitation process generates large volumes of low density sludge which are hard to dispose.

Sulfide precipitation is also effective in treating toxic heavy metal ions. The general idea is the same as hydroxide precipitation, with iron sulfide replacing calcium hydroxide. This process has some benefits over traditional hydroxide precipitation. Due to the lower solubility of metal sulfide, it allows for a wider pH range of operation. The produced sludge is also easier to process afterwards. However, there are potential problems with sulfide precipitation processes. When sulfide precipitants are in an acidic environment, H_2S fumes can be produced [6]. Thus it is important for any precipitation process to be done in neutral or basic mediums. Finally, sulfide precipitation seems to form colloidal precipitates that do not settle out as well as hydroxide precipitates.

Coagulation sedimentation

Coagulations can be employed to work alongside precipitation processes to better remove heavy metals from wastewaters. Coagulation means to neutralize the colloidal forces which keep particles apart, thus helping them settle out of solution. Coagulants used in industry are aluminum, ferrous sulfate, and ferric chloride, which can neutralize charges of colloidal particles. The coagulants are mixed with the heavy metals to form a precipitate suspension that settles out due to gravity. Since coagulation treatment is meant for hydrophobic colloids and suspended particles, it is not able to fully treat heavy metal wastewaters with dissolved heavy metal ions [6].

Membrane filtration

Many studies have applied the separation of heavy metals using membrane filtration. The mechanism behind this is simply using membranes that are selective barriers due to pore sizes being smaller than metal ions to filter and remove them. To prevent passage through pores that are bigger than the ions, the metal ions are processed before running through the membrane. The micellar enhanced ultrafiltration (MEUF) system was introduced in 1980 for this reason [6]. By adding surfactants to the wastewater above a critical micelle concentration, the surfactant molecules will aggregate into micelles which bind to the metal ions to form large structures. These large structures will be too large to pass through the membrane pores and can be easily filtered. The driving force for these membrane processes include differences in concentration, pressure, temperature, and special setups that use electrical potential [6].

Adsorption processes

Recognized more recently as a cheap and effective method for heavy metal removal, adsorption using different man-made and natural adsorbents has received a lot of attention lately. Adsorption is the adhesion of ions onto a surface due to electrostatic attraction, chemisorption, and/or van der Waals forces. The adsorption process can offer high quality heavy metal removal and the adsorbent can sometimes be regenerated and reused.

One type of adsorbent that is widely used are activated carbons. Activated carbons are a form of carbon usually from charcoal that has been processed by heat to

greatly increase its surface area. By activating the charcoal, one gram of activated carbon can have a surface area of 1300 m^2 [6]. This extremely large surface area works well with van der Waals forces to trap and remove heavy metals effectively. Currently coal based active carbon is expensive, thus much of the current research on active carbon is to find an inexpensive source for it. The second major problem is that activated carbon adsorption of heavy metals do not work very well in low concentration solutions. Studies have shown that in low concentrations of 1-100 mg/L, activated carbons can be ineffective [17].

In 1991, carbon nanotubes were discovered and have been widely studied for their many applications. For the process of adsorption, carbon nanotubes that have been modified show great potential for removing heavy metal ions dissolved in wastewaters, with maximum sorption capacities of 100 mg/g for lead [6]. The adsorption mechanisms for carbon nanotubes are a mixture of electrostatic attraction and chemical interaction. The modification used to increase adsorption capacities are HNO_3 and $KMnO_4$. These nanotubes show an even better adsorption capability than traditional activated carbons. Since these nanotubes are extremely expensive to manufacture and are not considered environmentally friendly, they are still not ideal for large scale heavy metal removal from wastewaters.

Medical chelation

Heavy metal chelation therapy is a medical treatment widely used in reducing the toxic effects of metals in human. Chelation is the bonding of ions and molecules to metal ions and involves the formation of coordinate bonds between ligands and metals that would then form a coordination complex. The idea is to use molecules with multiple ligands to bond with metal ions by donating electron pairs. The resulting complex structure would act as a trap that would help the body to excrete the toxic metal ions [18]. Chelating agents are compounds possessing ligands that would bond with metal ions to form complex ring-like structures called chelates [9]. The desired ligands are usually in chemical groups such as thiols, disulfide, amine, imine, hydroxyl, phosphate, and carbonyl groups. Many of the successful chelating agents contain 2 or more of these ligand groups that would form bonds with the metal ion creating a ring like structure. This is shown in Figure 1.

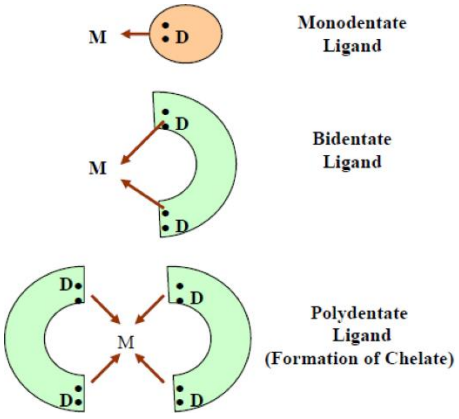

Figure 1. Chelation binding [9]

Currently the most used chelating agent is calcium disodium ethylenediamine tetraacetic acid (CaNa2EDTA) [9]. This is a form of ethylenediamine tetraacetic acid with bonds to sodium and calcium ions, seen here in Figure 2.

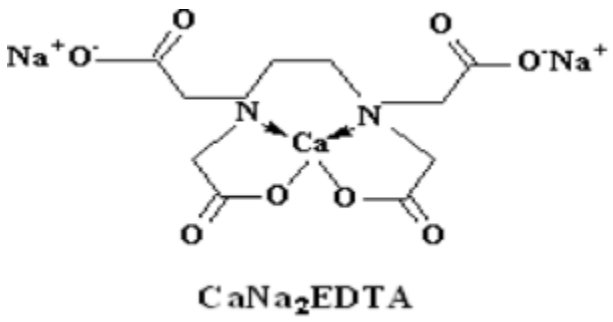

Figure 2. EDTA structure [9]

Since the 1950s, EDTA has been the main treatment for lead poisoning [18]. It is valuable in treating metal poisoning from metal species that have higher affinity than calcium. A metal species that has a higher stability constant than another species will remove the latter and take over the chelation complex [9]. A table of stability constants for EDTA is shown in Table 1.

Table 1. EDTA stability constants [9]

Table 1. EDTA-metal complex stability constants.

Metal	Na	Li	Ba	Sr	Mg	Ca	Mn	Fe	Co	Zn	Cd	Pb	Ni
K (log)	1.7	2.8	7.8	8.6	8.7	10.6	13.4	14.4	16.1	16.1	16.4	18.3	18.4

Since lead shows a much higher stability constant than calcium, CaNa2EDTA would chelate lead ions by replacing the Ca with Pb in the complex resulting in PbNa2EDTA, while leaving calcium in the body [9]. The calcium left behind in the body is relatively harmless, while the lead's harmful effects are nulified. Other chelators include D-Penicillamine (DPA), and Meso-2,3-Dimercaptosuccinic Acid (DMSA), both shown below in Figure 3.

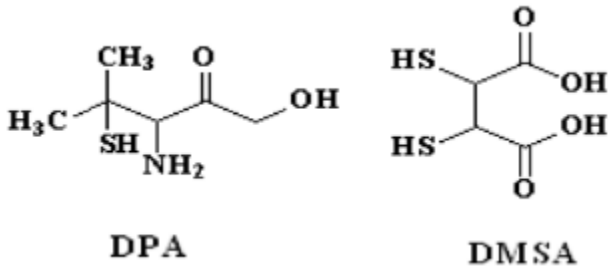

Figure 3. DPA and DMSA structures [9]

2.4 Hydrogel and functional groups used in this research

Poly(allylamine)

Poly(allylamine) (PAAm) is a polymer formed from linking allylamine groups with the structure shown below in Figure 4.

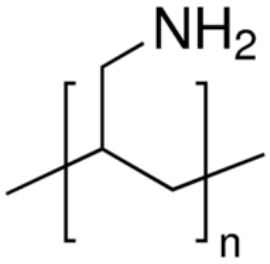

Figure 4. Poly(allylamine) structure [20]

These pertruding amine groups are metal chelating ligands that will form bonds with metal ions. These groups also form bonds with the carboxyl groups on DHBA and TGA. PAAm crosslinked hydrogels are soft and wet materials with three-dimensional crosslinked networks that can contain up to 90% water. This swelling effect is favorable for easy access of ions to the inside surfaces of the structure, making it a great compound to immobilize functional groups. PAAm, due to its amine groups, is also a pH-sensitive polymer, which will respond to changes in pH by varing its size. In this case, lowering the surrounding pH of a medium will cause PAAm to swell, which will help with releasing captured ion inside the structure.

DHBA and TGA

In nature, some enzymes called siderophores have a very high affinity towards binding with metal ions. The process for toxic metals to poison people is by attacking enzymes and replacing their naturally bounded metals. This is the exact process we seek to replicate. One siderophore we are interested in mimicing is enterobactin, which is a naturally occuring compound that has high affinity for metals [19]. 2,3-

Dihydroxybenzoic acid (DHBA) was chosen as a suitable substitute for enterobactin and studies have shown good metal sequestration using this [20]. DHBA is a natural phenol which is found abundantly in the lovi-lovi fruit of the Philippines, and is present in many siderophores [21]. Thioglycolic acid (TGA), which has a thiol and hydroxyl group, is similar to enzymes like cysteine and is chosen as the second compound to sequester heavy metals [20]. TGA is an organic compound that is usually a colorless liquid with a strong smell. It has many different uses, including hair removal, hair replacement, leather processing, and acidity indicator [21]. It will usually form metal complexes starting from its dianion form into a metal ring with various metals using its thiol and hydroxyl groups. These two different compounds will be the focus of our research on heavy metal sequestration as we test how well they are able to perform in different situations and what uptake model they follow.

2,3-Dihydroxybenzoic acid (DHBA) and Thioglycolic acid (TGA) are shown below in Figure 5.

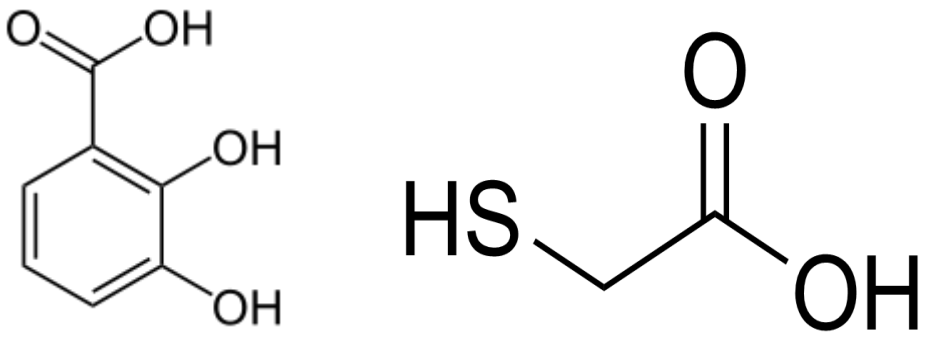

Figure 5. DHBA and TGA structures respectively [20]

The carboxyl groups shown in the structures are what binds with the amine groups on PAAm for functionalization. The chemical structures also show the metal-binding ligand groups. DHBA has 3 hydroxyl sites available for binding, with the primary chelation ligands being the two hydroxyl groups attached to the benzene ring. TGA has a thiol group and a hydroxyl group. These ligand groups coupled with the amine group that comes from PAAm should provide a good variety of sites for heavy metals to bind.

Ferrocyanide

On the radionuclide side of this research we will start by looking at an already established compound called Prussian blue (PB) and its uses as an antidote for certain kinds of heavy metal poisoning, including thallium and more importantly cesium-137. Prussian blue is a dark blue synthetic compound first made back in the 18^{th} century as a substitute for for expensive Lapis Lazuli coloring [10]. Its chemical formula is $Fe_4[Fe(CN)_6]_3$ with cage like chemical stuctures called ferrocyanide shown here in Figure 6.

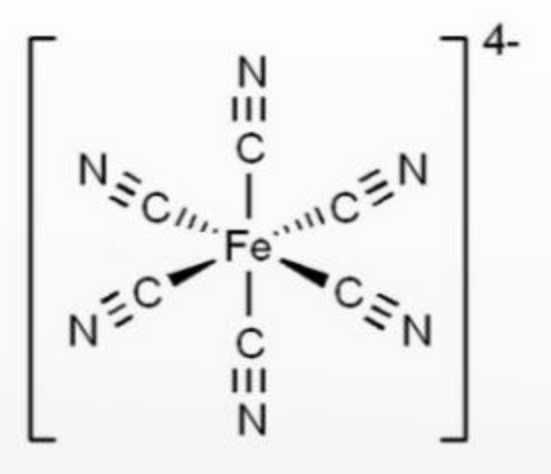

Figure 6. Ferrocyanide structure [23]

Each ferrocyanide group in Prussian blue has the ability to capture cesium ions. It is a simple crystal structure that has a cage size very close to the hydration radius of cesium at 3.25A [22]. Since this hydration radius is smaller than those of other predominant metals like Na, Ca, and Mg, it is able to deny capture of these bigger metals and be more selective towards cesium ions. In modern medicine, Prussian blue has been used for treating heavy metal poisoning and is notably used for adsorption of radioactive cesium after radioactive contamination accidents such as the Goiania accident in Brazil and Chernobyl disaster.

Studies have shown that PB nanoparticles have 2 general adsorption mechanisms used for cesium capture [10]. One is physical adsorption with the hydrated cesium being physically trapped by the lattice of the crystal structure shown in Figure 7.

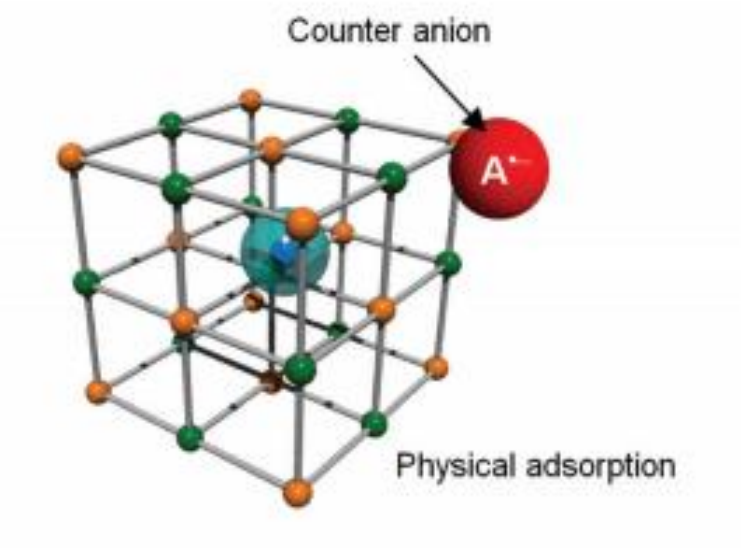

Figure 7. Ferrocyanide physical adsorption [23]

The other mechanism is chemical adsorption with proton-exchange achieved through defects in the lattice structure giving the lattice a presence of coordination water. Ishizaki et al. showed that prussian blue with high hydrophilic defect sites demonstrate better adsorption of cesium than low defect cases, with evidence to show that cesium was in fact trapped inside of the structure rather than just stuck to the surface [23]. In this research we will be using compounds of potassium ferrocyanide and sodium ferrocyanide to mimic the mechanisms of cesium ion entrapment. Ferrocyanide particles have been modified on other carriers such as biomass from algae and mesoporous silica with great success. The current adsorption capacities for these particles are around the range of 200 mg/g with only a few types that can be successfully recovered after the first time usage.

2.5 Modeling

Kinect modeling: pseudo-first-order and pseudo-second-order

If the modified hydrogels are going to be used for large scale water cleanup, studying adsorption speeds are going to be important in providing insight on designs. Adsorption kinetics is the basic study of adsorption rates and capacities. Kinetic models correlate adsorption amounts vs. time and can calculate equilibrium adsorption capacities and adsorption constants. In this study, we will be comparing our kinetic testing with the two most popular adsorption models, the pseudo-first-order (Lagergren model) and pseudo-second-order (Ho model).

In 1898, Lagergren presented a first-order rate equation for describing liquid-solid phase adsorption of oxalic acid and malonic acid onto charcoal [24]. The model is a correlation between its adsorption capacities. The basic rate reaction he presented was

$$\frac{dq_t}{dt} = k_1(q_e - q_t) \quad (1)$$

Where:

q_t= Adsorption capacities at time t (mg/g)

q_e= Adsorption capacities at equilibrium (mg/g)

k_1= First order rate constant (1/min)

Expressed in its linear form, the equation becomes:

$$\log(q_e - q_t) = \log q_e + \frac{k_1}{2.303} t \quad (2)$$

By fitting experimental data to this equation and plotting a line with $\log(q_e - q_t)$ vs.t, we are able to get the slope and intercept, solving for k_1 and matching q_e. If the plotted line is relatively linear, it would signify that the adsorption reaction is following pseudo-first-order kinetics. In many cases in the past, the pseudo-first order equation has not fit very well with experimental data after the initial few minutes of contact [25].

In 1995, Dr. Ho presented the pseudo-second-order kinetic model for adsorption of divalent metal ions onto peat [26]. The main assumptions for the adsorption process is that it is a second-order reaction with the rate-limiting step being chemical adsorption. Over the years, this model has been widely applied to many studies of adsorption including lead, nickel, arsenic, and dyes. The equation for this model is given below:

$$\frac{dq_t}{dt} = k_2(q_e - q_t)^2 \quad (3)$$

Which can then be linearized into:

$$\frac{t}{q_t} = \frac{1}{k_2 q_e^2} + \frac{t}{q_e} \quad (4)$$

Where:

q_t= Adsorption capacities at time t (mg/g)

q_e= Adsorption capacities at equilibrium (mg/g)

k_2= Second order rate constant (g/ (mg min))

By fitting experimental data to this model equation and plotting a line with t/q_t vs. t, we can get the slope and intercept, solving for k_2 and q_e. If the plotted line is linear, it would signify that the adsorption reaction is following pseudo-second-order kinetics.

Isotherm modeling: Langmuir, Freundlich, and Temkin

An adsorption isotherm is a semi-empirical model that shows the relationship between the concentration of an adsorbate solution versus the amount adsorbed onto the adsorbent at a constant temperature. Isotherms only describe the equilibrium state, which will give insight on how the adsorbate and the adsorbent interact. Since adsorption amounts are directly related to the concentration of adsorbates, isotherm experiments are done by preparing adsorbate solutions with different initial concentrations and seeing how much is adsorbed [27]. In our research we will be looking at three different isotherm models that have been widely used in the field of adsorption research.

The first model is Langmuir's model derived by Irving Langmuir in 1918. This was the first scientifically based isotherm derived from the idea of gases adsorbed onto solid surfaces [27]. The semi-empirical derivation was based on three general assumptions [28]:

1. All adsorption sites are equal and can bond with one molecule
2. The surface is homogeneous and adsorbed molecules do not interact
3. At maximum adsorption, only a monolayer is formed. No adsorption between adsorbates

Based on these assumptions and reaction kinetic definitions, Langmuir presented the following equation:

$$q_e = \frac{q_{max} K_L C_e}{1 + K_L C_e} \quad (5)$$

Where:

q_e= Amount of metal adsorbed per gram of adsorbent at equilibrium (mg/g)

q_{max}= Maximum amount of metal that can be adsorbed onto adsorbent (mg/g)

K_L= Langmuir isotherm constant (L/mg)

C_e= Equilibrium concentration of adsorbate (mg/L)

The equation can be transformed into its linear form:

$$\frac{\mathbf{1}}{\boldsymbol{q_e}} = \frac{\mathbf{1}}{\boldsymbol{q_{max}}} + \frac{\mathbf{1}}{\boldsymbol{q_{max} K_L C_e}} \quad (6)$$

By plotting the values of $1/q_e$ vs $1/C_e$ from experimental data sets, model parameters of q_{max} and K_L can then be calculated from the slope and intercept. Matching experimental data to the model and calculating a regression R^2 will show if the adsorption process follows Langmuir isotherms.

Secondly, we have the Freundlich adsorption isotherm proposed in 1909 by Herbert Freundlich [27]. This isotherm equation is purely empirical in matching experimental data. The model has been used to describe adsorption characteristics of heterogeneous surfaces as opposed to the homogeneous surfaces from the Langmuir Isotherm. The Freundlich model assumes that many different types of active binding sites are acting at the same time, such as different ligands on a metal binding molecule [29]. The model equation is given below:

$$\boldsymbol{Q_e = K_f C_e^{\frac{1}{n}}} \quad (7)$$

Where:

Q_e= Amount of metal adsorbed per gram of adsorbent at equilibrium (mg/g)

K_f= Freundlich isotherm constant (mg/g (L/mg) $^{1/n}$)

C_e= Equilibrium concentration of adsorbate (mg/L)

n= Adsorption intensity

Here the K_f and n factors are Freundlich parameters. K_f is a direct indicator of the maximum adsorption capacity, while n indicates how heterogeneous an adsorption process is. As the value of n becomes greater than 1, it is expected to have greater surface heterogeneity [28]. The Freundlich equation can be linearized into the following:

$$\boldsymbol{logQ_e = logK_f + \frac{1}{n} logC_e} \quad (8)$$

The Freundlich parameters K_f and n can be easily calculated by fitting experimental data into a $logQ_e$ vs $logC_e$ plot and calculating the slope and intercept. Calculating a linear regression R^2 will show how well experimental data matches with the Freundlich isotherm.

Finally, we have the Temkin isotherm model. The Temkin isotherm model was originally used to describe the adsorption of hydrogen onto platinum electrodes within acidic solutions, and considers the effects of indirect adsorbate and adsorbate interactions [29]. The model equation is given below:

$$\boldsymbol{q_e = \frac{RT}{b} \ln(A_T C_e)} \quad (9)$$

Which can be linearized into:

$$\boldsymbol{q_e = \frac{RT}{b} \ln(A_T) + \frac{RT}{b} \ln(C_e)} \quad (10)$$

Where:

q_e= Amount of metal adsorbed at equilibrium (g/g)

R= Universal gas constant (8.314 J/mol/K)

T= Temperature (K)

b= Temkin isotherm constant (J/mol)

A_T= Temkin isotherm equilibrium bind constant (L/g)

C_e= Concentration at equilibrium (g/L)

By plotting q_e vs $\ln(C_e)$, the Temkin parameters of RT/b and A_T can be calculated from the slope and intercepts. Calculation of the linear regression R^2 will show how well experimental datasets match with the Temkin model.

3. MATERIALS AND METHODS

This research was divided into two parts, the first was toxic metals testing, the second was cesium testing. Dr. Zahra Mohammadi synthesized and quantified all of the hydrogels following the procedures set in her dissertation [20]. The experiments performed in this study are binding tests with different concentrations to match isotherm models, kinetic tests to match kinetic models, selectivity tests, pH tests, reusability tests, and finally column studies to see how well the gel worked in a steady state environment.

3.1 Reagents

Poly(allylamine hydrochloride) (PAAm) with an average molecular weight of 56 kDa, N,N'- methylenebisacrylamide (MBA), Potassium Ferrocyanide, and Sodium Ferrocyanide were obtained from Sigma-Aldrich. 2,3 dihydroxybenzoic acid (DHBA), thioglycolic acid (TGA), N,N,N -triethylamine (TEA), and dimethylformamide (DMF) were obtained from Fisher Scientific. All metal chlorides were obtained from Fisher Scientific. Dicyclohexylcarbodiimide (DCC) and N-hydroxysuccinimide (NHS) were obtained from Fisher Scientific. Deionized water (DI) was from EMD Millipore water purifier.

3.2 Analysis equipment

All mono- and multi-elemental analysis of our samples in this research were done using the Inductively Coupled Plasma Optical Emission Spectrometry (ICP-OES)

instrument. The ICP-OES is a two-part spectroscopy analyzer used for the detection of trace amounts of metals. The ICP-OES system is split into two sections, the inductively coupled plasma section and the atomic emission spectroscopy section. Both sections are shown in Figure 8.

Figure 8. Picture of the ICP-OES with sections shown

First the ICP uses argon gas and an intense electromagnetic field to create super-heated plasma at temperatures of around to 7000 K. A pump then delivers a fluid sample into an analytical nebulizer that transforms the liquid into mist and sends it into the plasma. The plasma will then heat the sample and break it down into atoms and charged ions which then reform and emit light at different wavelengths. The OES system has

lenses that to focus the emitted light on a diffraction grating to separate the wavelengths for the optical spectrometer to read. The spectrometer detects the intensities of these wavelengths and develops a calibration curve. It then compares the intensity to the curve and calculates concentrations of desired metals based on interpolation. Using this instrument, we were able to accurately analyze our samples of cadmium, arsenic, lead, cesium, and any other competing metals.

3.3 Synthesis process for As, Cd, and Pb hydrogels

The general synthesis process for heavy metals ion adsorption hydrogels was performed by Dr. Mohammadi following her previous paper and dissertation [8, 20] and can be summarized into the following. A 20% polymer solution containing MBA was prepared. Cross-linker was dissolved in DI water with TEA and added to the polymer solution. This mixture was transferred into small vials and held at ambient temperatures and then cooled. Then the hydrogels were removed and washed with sodium chloride solution. These steps provided the unconjugated PAAm hydrogels. Next, a solution of either TGA and NHS or TGA, DHBA, and NHS in DMF solution was mixed with a solution of DCC in DMF solution. This mixture was stirred to form a precipitate. The precipitate was filtered and added onto the PAAm hydrogel. This end product was allowed to sit and stabilize, then washed with DI water. The resulting 3 heavy metal adsorption hydrogels used in our experiments were PAAm, PAAm/TGA abbreviated into PT, and PAAm/TGA/DHBA abbreviated into PTD.

3.4 Synthesis process for Cs hydrogels

The synthesis process for cesium adsorption hydrogels was also performed by Dr. Mohammadi following her previous works [8, 20]. A 20% polymer solution containing MBA was prepared. Cross-linker was dissolved in DI water with TEA and added to the polymer solution. This mixture was transferred into small vials and held at ambient temperatures and then cooled. Then the hydrogels were removed and washed with sodium chloride solution. These steps provided the unconjugated PAAm hydrogels. Next, a solution of DHBA and NHS in DMF solution was mixed with a solution of DCC in DMF solution. This mixture was stirred to form a precipitate. This precipitate was filtered and added onto the PAAm hydrogel. This end product was allowed to sit and stabilize, then washed with DI water. This part had several different mass ratios of DHBA to Hydrogel. After all of that, different amounts of potassium ferrocyanide and sodium ferrocyanide salt were added to the gel mass. The gels were filtered and washed several times again. Table 2 shows all 24 combinations of DHBA, hydrogel and salt:

Table 2. DHBA and salt ratios for cesium adsorption hydrogels

36.21 % Wt DHBA/gel		51.49 % Wt DHBA/gel		2.65 % Wt DHBA/gel	
Sodium Ferrocyanide (Wt %)	Potassium Ferrocyanide (Wt %)	Sodium Ferrocyanide (Wt %)	Potassium Ferrocyanide (Wt %)	Sodium Ferrocyanide (Wt %)	Potassium Ferrocyanide (Wt %)
10%	10%	10%	10%	10%	10%
20%	20%	20%	20%	20%	20%
40%	40%	40%	40%	40%	40%
60%	60%	60%	60%	60%	60%

These 24 combinations were tested using selectivity tests and concentration binding tests to determine the optimum recipe.

3.5 Varying concentration binding tests for isotherms

To obtain experimental data to match with adsorption isotherms, all hydrogels were tested using solutions of metal ions with different initial concentrations. $CdCl_2$, $AsCl_3$, and $PbCl_2$ were used to make 10 ml solutions of concentrations of 5, 20, 50, 100, 200 and 400 ppm prepared in 20 ml glass vials. For CsCl, 10 ml of concentrations of 50, 100, 200, 500 and 1000 ppm were prepared in 20 ml glass vials. All solutions were adjusted to the pH of 7.5. Next 5 mg of hydrogel were added to the solutions and the vial was held at room temperature for 2 hours to equilibrate. Finally, after filtration, the filtrate was taken to ICP-OES for analysis of concentration.

Isotherm models were then employed to try and match with the experimental data sets to better understand how the liquid and hydrogel phases reached equilibrium. The isotherm used were Langmuir, Freundlich, and Temkin models. The model parameters were calculated by plotting the experimental data according to the models to determine the slope and intercepts. The accuracy of each model was determined by a linear regression coefficient.

3.6 Kinetic binding tests

To match with kinetic models, the hydrogels were tested using differing adsorption times. 30 ml of $CdCl_2$, $AsCl_3$, and $PbCl_2$ solutions at 2000 ppm were prepared in a 50 ml glass beaker. For CsCl, 30 ml of 500 ppm were prepared in a 50 ml glass beaker. All solutions were adjusted to the pH of 7.5. Next, 30 mg of hydrogel was added to the beakers. At the time steps of 1, 5, 10, 20, 40, 60, 120, 180, 240 minutes, samples from the solution were taken and stored. Finally, the samples were taken to be analyzed by ICP-OES for concentrations.

Kinetic models were then employed to try and match with the experimental data sets to better understand how the dissolved ions in the liquid interacted with the surfaces of the hydrogel. The kinetic models used were the pseudo-first-order (lagergren model) and pseudo-second-order (ho model) models. The model parameters were calculated by plotting the experimental data according to the models and determining the slope and intercepts. The accuracy of each model was determined by a linear regression coefficient.

3.7 Selectivity tests

Since the usage of these hydrogels is meant for oil production waters and industrial wastewaters, they must be able to function efficiently in solutions with competing metal ions. The selectivity of these hydrogels was tested by introducing competing ions in solutions. For heavy metal hydrogels, three 30 ml solutions of Pb, Cd, As, Fe, Cu, and Zn at 1000ppm were prepared in a 50 ml beaker. 30 mg of hydrogel was

added to the solution and allowed to sit at room temperature and reach equilibrium for two hours. Then samples of the solution were taken to the ICP-OES for analyses of the metal concentrations.

For the cesium hydrogels, selectivity tests were done as the first step after synthesis to identify which combination of base hydrogel, DHBA, and salt would adsorb the most cesium. The selectivity tests were done on a molar basis. 10 ml solutions of CsCl at 0.1 mMolar were mixed with 0.1, 0.5, 1, 2, 3 mMolar of NaCl and KCl in 20 ml glass vials. These molar values were roughly 6 ppm, 30 ppm, 60 ppm, 120 ppm, and 180 ppm. Then 10 mg each of the original 24 recipes of hydrogels were added to the selectivity solutions with a total of 240 tests being performed. Each test was done at room temperature with two hours of incubation time. Afterwards, the solutions were taken to be tested by ICP-OES for concentration readings.

3.8 pH tests

The pH of the solution medium was very important in our adsorption process and needed to be tested. In Dr. Mohammadi's dissertation, all of the batch experiments were performed at pH of 2.5. In this study, the batch experiments were performed at 7.5. To establish a relationship between these results, tests were performed to determine pH's effects on adsorption capacities. In these tests, solutions of varying pH at 1.5, 3.5, 5.5, and 7.5 were prepared by adjusting 10 ml solutions of Cd, As, Pb at 2000 ppm and Cs at 500 ppm in 20 ml glass vials with 0.1M HCl and 0.1M NaOH. 5 mg of each hydrogel was added to these solutions in room temperature and let sit for two hours. Afterwards,

the solutions were taken to be tested by ICP-OES for concentration readings to see how well the hydrogels adsorbed the contaminants in different pH environments.

3.9 Reusability tests

For these hydrogels to be economical, they should be reusable. In literature, desorption of heavy metals was usually achieved through the usage of low pH acids. Prussian blue and other ferrocyanide compounds, on the other hand, have always had problems with recoverability, but we decided to use the same recovery procedure as the heavy metal hydrogels on our cesium hydrogels to see if it will have any effect. In our procedures, we saturated our 10 mg hydrogels by putting them in 10 ml of 2000 ppm solutions of Cd, As, Pb and 500 ppm for Cs at room temperature just like previous experiments. After 2 hours of stabilization, the hydrogels were filtered out of solution, washed with DI water, and then put into 10 ml of 1 M HCl to desorb the contaminants from the hydrogel for 1 hour. The hydrogels were rinsed after the acid with DI water and again added to 10 ml of the same solutions as before. This cycle was repeated five times and each time the solutions are taken to the ICP-OES for analysis.

3.10 Column study

The final tests for these hydrogels were the column studies. Due to all previous testing being batch tests, it was important to have a general idea on how high adsorption can be in a steady state environment with a flowing current. Only through these tests could we know how well the hydrogels deal with flowing waters, short contact times

with solutions, and how to scale up for treating industrial sized wastewaters. The general setup for the column study with a syringe pump, packed column, and sample collector is shown in Figure 9.

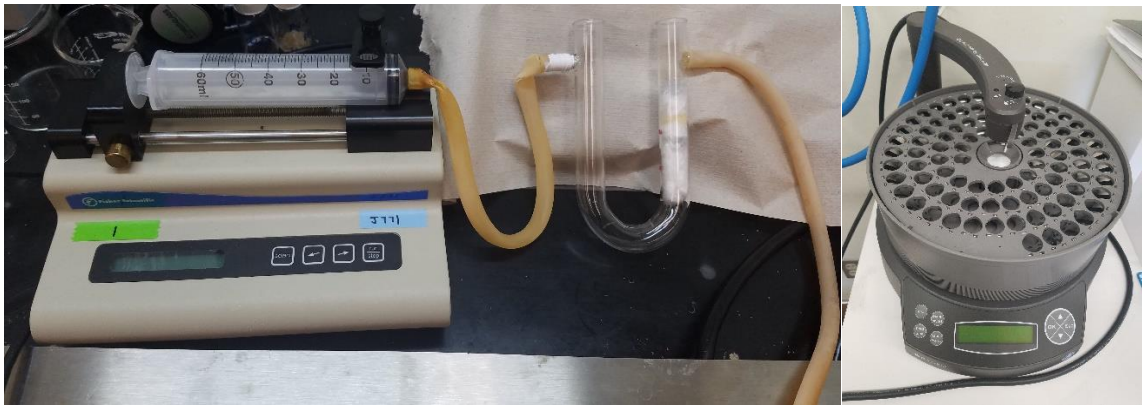

Figure 9. Column study setup

A solution of each heavy metal contaminant at 4000 ppm and 1000 ppm of cesium was pumped by a syringe pump at the flow rate of 120 ml/hour. The solution was pumped into a rubber hose and into the 0.5-inch diameter glass U-column. On the right side of the column, glass beads and glass fibers were used to support and hold 200 mg of hydrogel, approximately 1.5 mm thick, that covers the entire cross section of the column. The solution was pumped through this column to the right side where it was collected in a frac-920 sample collector. The concentrated solutions were immediately followed by 240 ml of DI water to flush any remaining contaminant out of the column. The sample collector collected 5 ml samples that were then all taken to the ICP-OES for analysis.

4. RESULTS AND DISCUSSION

4.1 Gel synthesis

Following previous literature procedures from Dr. Mohammadi's dissertation, polyallylamine hydrogel was synthesized by Dr. Mohammadi. Molar ratio of 0.5 % of DHBA and TGA were shown to be optimum in her dissertation and thus used to conjugate the heavy metal hydrogels. Since this is the first time we were experimenting with Cs adsorption hydrogels, we must determine the best weight ratios for DHBA and the two salts of sodium ferrocyanide and potassium ferrocyanide. To determine the optimum ratio, 24 combinations of Cs adsorption hydrogels were synthesized. These recipes are shown here in Table 3:

Table 3. DHBA and salt ratios for cesium adsorption hydrogels

36.21 % Wt DHBA/gel		51.49 % Wt DHBA/gel		2.65 % Wt DHBA/gel	
Sodium Ferrocyanide (Wt %)	Potassium Ferrocyanide (Wt %)	Sodium Ferrocyanide (Wt %)	Potassium Ferrocyanide (Wt %)	Sodium Ferrocyanide (Wt %)	Potassium Ferrocyanide (Wt %)
10%	10%	10%	10%	10%	10%
20%	20%	20%	20%	20%	20%
40%	40%	40%	40%	40%	40%
60%	60%	60%	60%	60%	60%

4.2 Selectivity tests

The selectivity of the heavy metal adsorption hydrogels was tested using a solution containing Pb, Cd, As, Fe, Cu, and Zn at 1000ppm. The adsorption data is shown in the graphs of Figure 10.

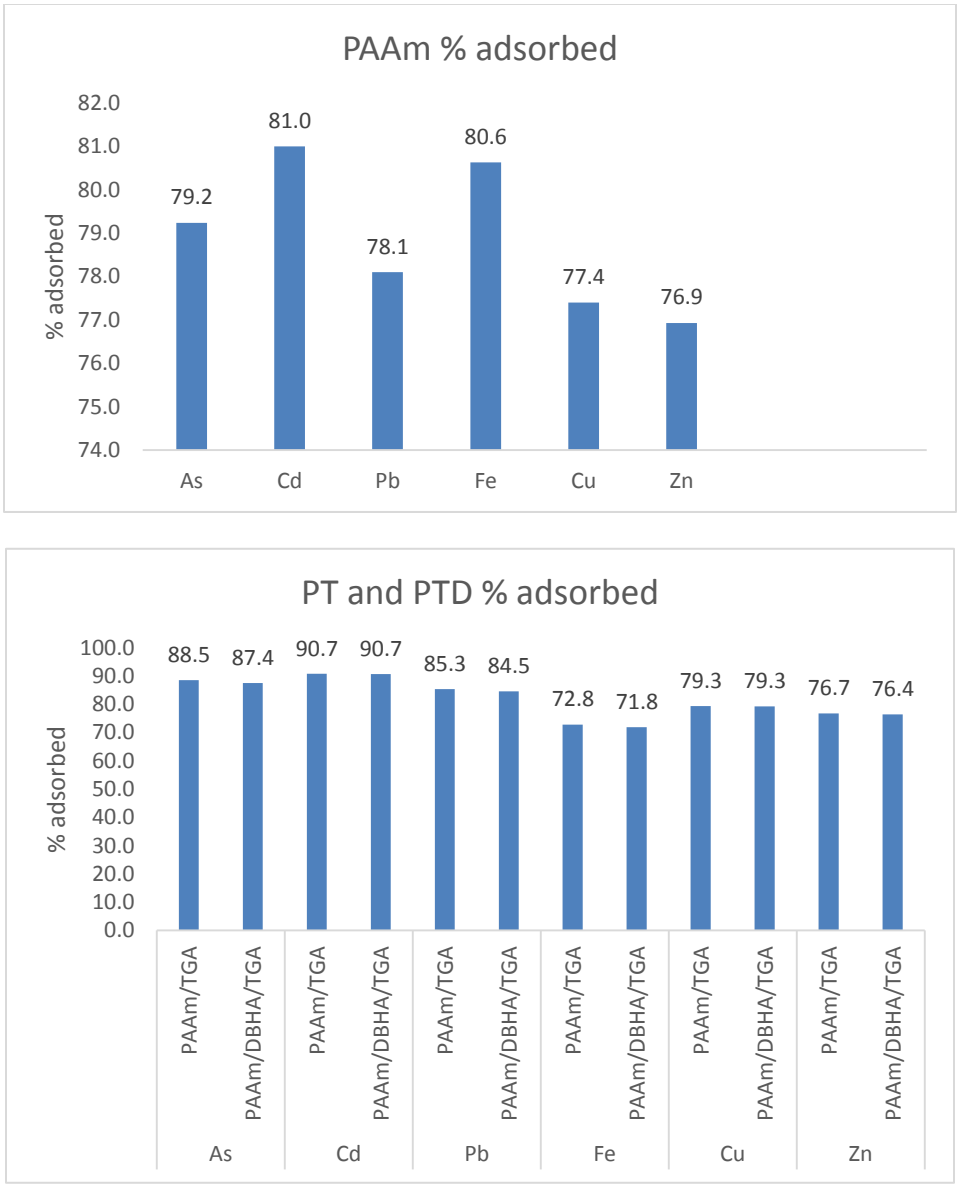

Figure 10. Selectivity adsorption % for heavy metal hydrogels

As the graphs show, PAAm/TGA and PAAm/DHBA/TGA have similar results in selectivity with very little differentiation from each other. But compared to the basic PAAm hydrogel, a decrease in affinity for iron can be seen from both modified hydrogels. The results also show that our target heavy metals of cadmium, lead, and arsenic are currently the most adsorbed contaminants from the solution. The decrease in iron adsorption is important because iron is the primary competing metal in wastewater streams. These selectivity results are good for practical applications and are comparable to other adsorption compounds from literature. Bio-carbon and functionalized clays research from literature showed a natural affinity to cadmium and lead over copper and zinc with similar margins of difference at 5% to 10% [33] [34].

For Cs adsorption hydrogels, selectivity was done as the first test to differentiate between all of the 24 combinations of DHBA, salt type, and salt ratios. In our experiments, 240 tests were performed on the hydrogels to test how well they would adsorb Cs ions in the presence of NaCl and KCl in solution. These tests were carried out by varying the concentrations of the competing salts to see how they would change the adsorption of the hydrogels. From the ICP-OES results, it was shown that some of the hydrogel recipes showed extreme selectivity to cesium even in the presence of high concentration of competing salts. The average cesium adsorption in 1:1 molar ratio solutions for the all tests was around 55%, with Na adsorption averaging around 48% and K adsorption averaging around 44%. Out of these 24 recipes, 6 recipes were chosen for their high adsorption of cesium. The results for these 6 in 1:1 molar solutions are shown in Table 4.

Table 4. Six best recipes for cesium adsorption

recipe #	DHBA wt %	salt type	salt wt %	Cesium uptake %	Na uptake %	K uptake %
1	51.49	Potassium Ferrocyanide	10	62	44	42
2	51.49	Potassium Ferrocyanide	20	65	49	44
3	51.49	Potassium Ferrocyanide	40	61	42	43
4	51.49	Potassium Ferrocyanide	60	60	42	42
5	3	Sodium Ferrocyanide	60	66	43	43
6	3	Sodium Ferrocyanide	10	65	42	48

These 6 recipes were shown to have the highest percentage cesium uptake. They show that these hydrogels do possess selectivity for cesium in the presence of sodium and potassium ions. The 15% - 20% difference in adsorption percentages between cesium and the competing metals are also observed in other ferrocyanide cesium research papers, such as copper ferrocyanide on mesoporous silica and biomass functioned with ferrocyanide [35] [36].

4.3 Varying concentration binding tests for isotherms

The amount of contaminant adsorbed by the hydrogels is directly related to the initial concentrations of contaminants. To study the relationship between the adsorbate concentration and the adsorbent, experimental test data was matched to Langmuir, Freundlich and Temkin isotherms. Each heavy metal concentration was recorded using ICP-OES and used to calculate isotherm parameters. All three heavy metal hydrogels showed a much better fitting with the Freundlich model over the other two models.

Langmuir and Temkin isotherms did not fit well and generally had regression values below 70%. In these cases, the Langmuir isotherms would sometimes give a straight line when fitted, but often gave a negative intercept value. This negative intercept would result in negative parameters, suggesting that Langmuir adsorption is not correct. In Dr. Mohammadi's dissertation, she also observed negative Langmuir parameters [20]. Table 5, Table 6, and Table 7 show model parameters calculated from our data. The important numbers here are the Freundlich model parameters.

Table 5. Isotherm parameters calculated for PAAm

PAAm			
Langmuir isotherm			
Heavy metals	q_{max}	k_L	R^2
As	66.23	12	0.67
Pb	-79.51	-37.6	0.71
Cd	29.78	-8.56	0.78
Freundlich isotherm			
	n	k_f	R^2
As	0.721	9654.99	0.95
Pb	0.679	649.81	0.93
Cd	0.655	1081.05	0.97
Temkin isotherm			
	A	RT/B	R^2
As	191.57	72.65	0.64
Pb	55.32	79.21	0.48
Cd	98.87	54.32	0.59

Table 6. Isotherm parameters calculated for PT

PAAm/TGA			
Langmuir isotherm			
Heavy metals	q_{max}	k_L	R^2
As	-46.51	-43	0.69
Pb	51.81	-9.19	0.64
Cd	-59.52	-10.5	0.75
Freundlich isotherm			
	n	k_f	R^2
As	0.980	14078.44	0.96
Pb	1.052	806.5775	0.98
Cd	1.109	1159.449	0.95
Temkin isotherm			
	A	RT/B	R^2
As	261.73	94.374	0.86
Pb	75.22	61.737	0.77
Cd	82.62	67.611	0.79

Table 7. Isotherm parameters calculated for PTD

PAAm/TGA/DHBA			
Langmuir isotherm			
Heavy metals	q_{max}	k_L	R^2
As	-53.76	-46.5	0.77
Pb	434.78	2.3	0.79
Cd	166.67	-4.61	0.67
Freundlich isotherm			
	n	k_f	R^2
As	1.078	14256.95	0.94
Pb	1.047	544.57	0.94

Table 7. Continued

Cd	1.192	1198.47	0.92
Temkin isotherm			
	A	RT/B	R^2
As	221.56	95.77	0.68
Pb	36.60	80.00	0.81
Cd	82.41	61.11	0.80

Freundlich isotherm model can accommodate both uniform and multiple types of binding sites all acting at the same time. Each of these sites can have different energies of adsorption. In this case, the modified hydrogels have a few different ligand binding sites such as sulfur and oxygen groups from the modifications as well as amine groups from PAAm. The n parameter signifies the degree of surface heterogeneity. In the case of base PAAm hydrogel, the n value is lower than 1 signifying a lack of heterogeneity in binding [28]. The modified gels displayed n values slightly above 1, signifying that the surface of the hydrogel has different binding site types but is not extremely diverse. K_f parameters are an indication of maximum adsorption capacity [28]. A higher K_f value means higher adsorption capacity.

For cesium adsorption, the 6 hydrogel recipes that were previously chosen were further tested and evaluated using adsorption isotherms. The best and worst results are shown in Table 8 and Table 9.

Table 8. Best case recipe #2

Best case			
Langmuir isotherm			
Heavy metals	qmax	k_L	R^2
Cs	-303.03	-16.5	0.835
Freundlich isotherm			
	n	K_f	R^2
Cs	0.934	4871.221	0.9914
Temkin isotherm			
	A	RT/B	R^2
Cs	240.05	243.32	0.7015

This base case adsorption was achieved using recipe #2 out of the 6 recipes, which had adsorbed 68% of the original cesium in solution. The adsorption amount for recipe #2 is slightly higher than recipes #3 and #4, while being much higher than recipe #1. This suggests that 20% weight percentage of ferrocyanide is the optimum weight.

Table 9. Worst case recipe #6

Worst case			
Langmuir isotherm			
Heavy metals	qmax	k_L	R^2
Cs	-272.03	-12.2	0.789
Freundlich isotherm			
	n	K_f	R^2
Cs	0.937	4170.12	0.9895
Temkin isotherm			
	A	RT/B	R^2
Cs	214.816	229.32	0.719

The worst case results were obtained from recipe #6, which adsorbed 8% less cesium ions than the recipe #2. All 6 recipes had similar isotherm regression values and showed a good match with the Freundlich isotherm model. For the sake of time and effort, since recipe #2 had the best results so far, all future testing on cesium adsorption was done with this particular hydrogel recipe.

4.4 Kinetic binding tests

Kinetic testing is critical for understanding how to scale up these hydrogels to be used in large scale steady state adsorption of contaminants. We must know how quickly they can adsorb contaminants to accurately perform scale-up calculations. This kinetic testing will also give us valuable data useful for matching kinetic models, which can be used to estimate future adsorption studies based on contact time.

The heavy metal hydrogels showed extremely rapid adsorption of the targeted three heavy metals. The solutions used in these experiments are 2000 ppm for heavy metals and 500 ppm for cesium. Cd, As, and Pb solutions all had nearly complete adsorption in less than 5 minutes of contact time. Below in Figure 11, Figure 12, and Figure 13 are graphs of adsorption vs time for PAAm, PT, and PTD.

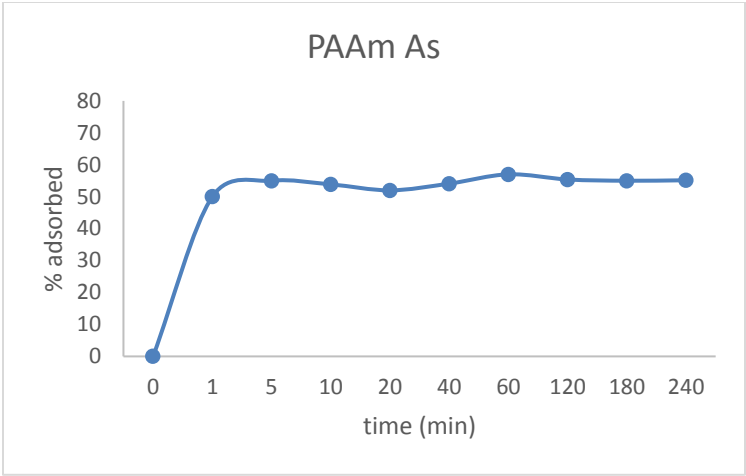

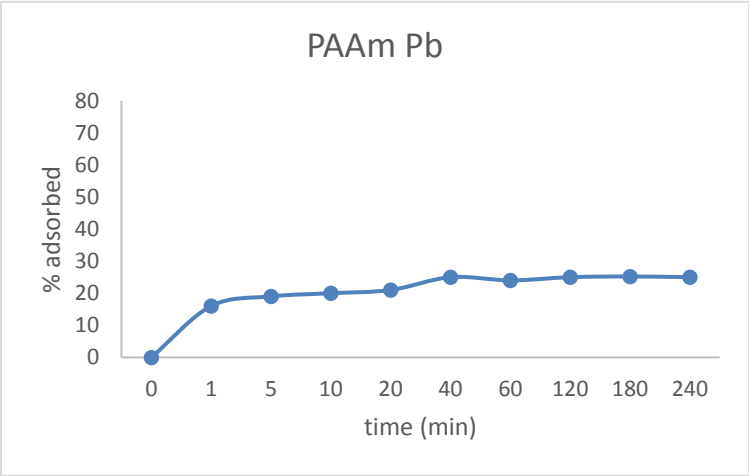

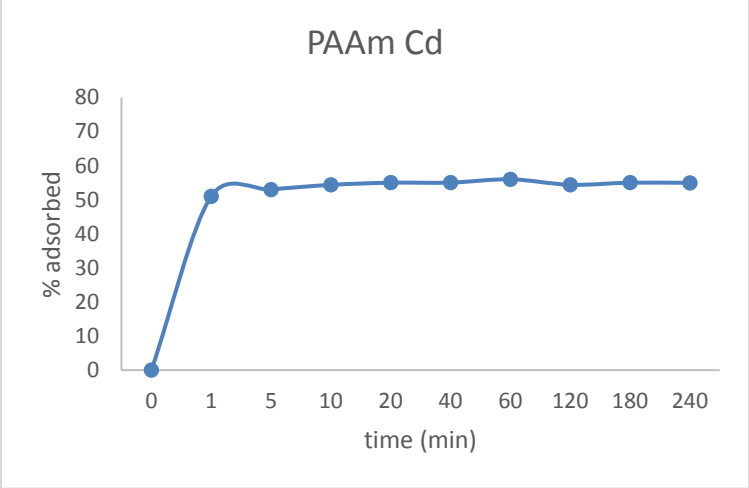

Figure 11. PAAm Kinetic adsorption results

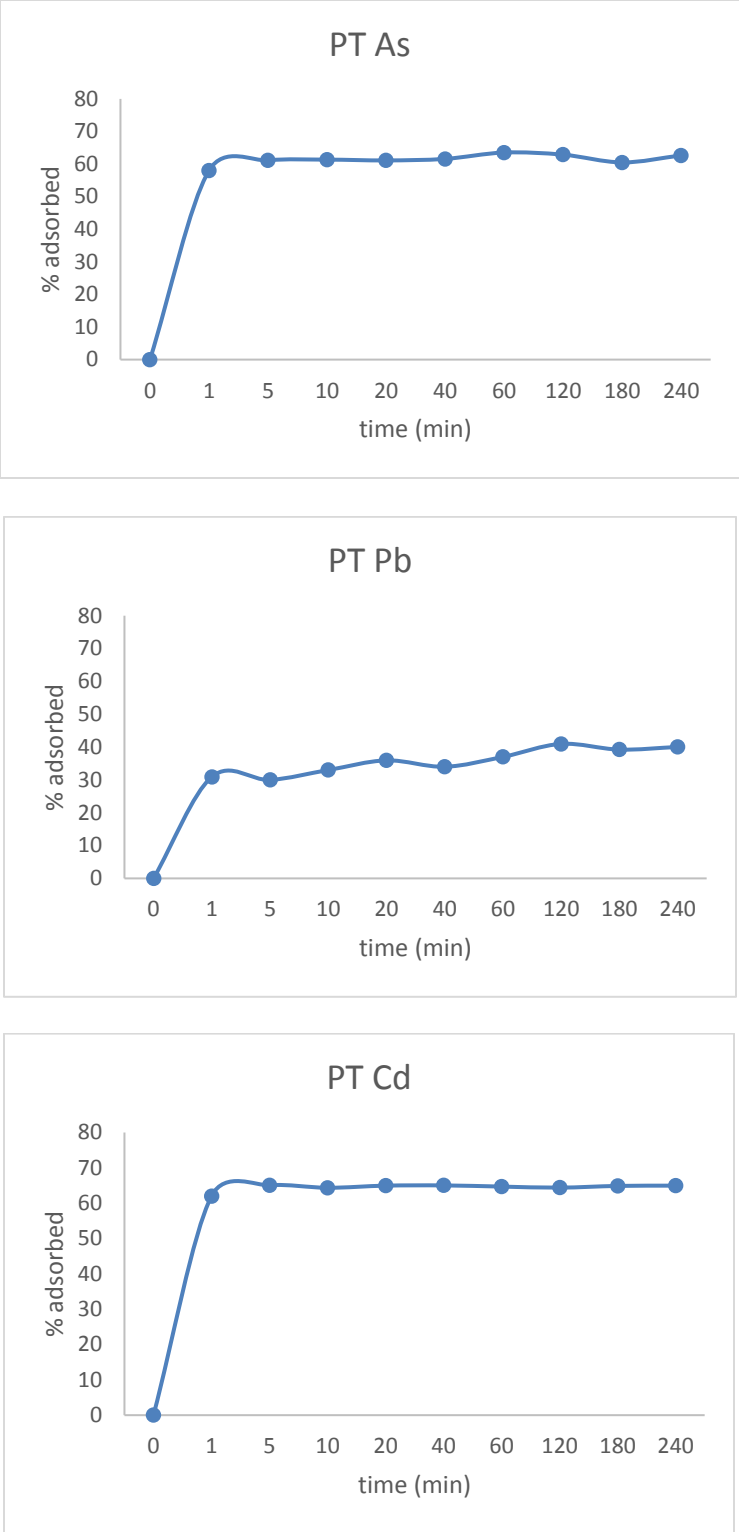

Figure 12. PT Kinetic adsorption results

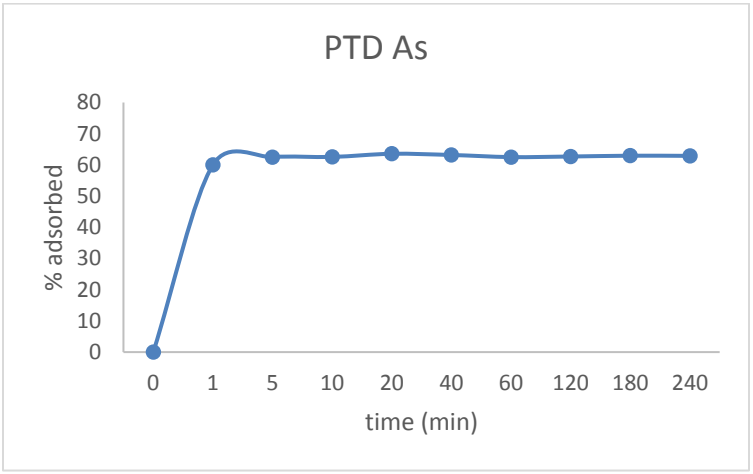

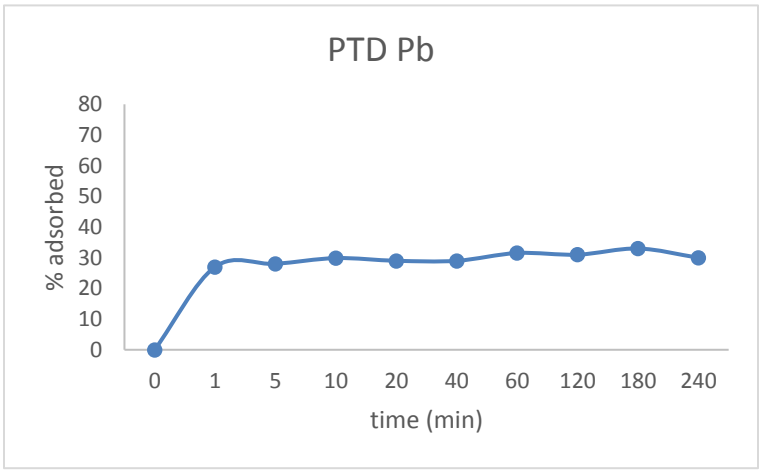

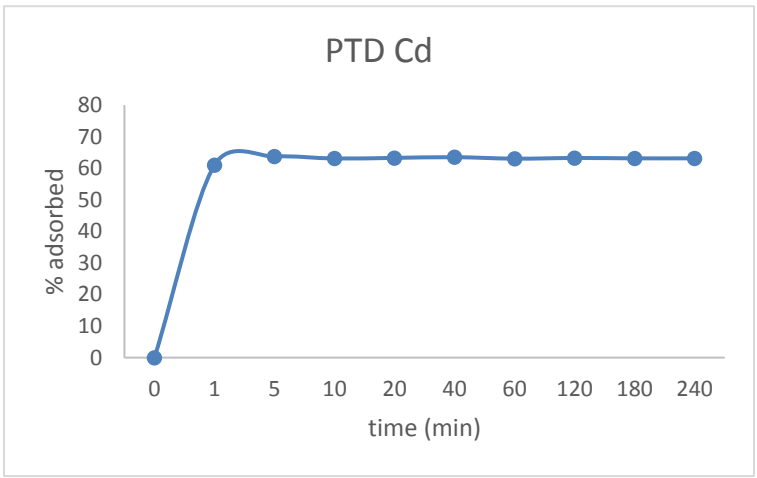

Figure 13. PTD Kinetic adsorption results

All three hydrogels showed extremely rapid adsorption in the kinetic tests. From these plots it can be seen that the hydrogels conjugated with DHBA and TGA showed less adsorption than the ones conjugated only with TGA. This could be due to the fact that sulfur ligand groups, which seem to show stronger affinity for heavy metals, are more numerous in the PAAm/TGA hydrogels. Also like previous results, PAAm showed significant adsorption but had the least amount of adsorbed out of the three.

The data sets were matched with pseudo first and second order kinetics. Pseudo-first order model did not match the data well and had low regression values. Pseudo-second order model did match the data well and regression values were close to unity. Table 10 shows pseudo second order kinetic model generated maximum adsorption capacities q_e and constants K_2 values:

Table 10. Pseudo-second order kinetic results for heavy metal adsorption

Pseudo Second order model						
	PAAm		PT		DPT	
As	q_e	709.09	q_e	911.1	q_e	878.2
	k_2	17.28	k_2	NA	k_2	0.027
Pb	q_e	434.78	q_e	566.67	q_e	476.19
	k_2	0.00035	k_2	0.00041	k_2	0.0044
Cd	q_e	669.09	q_e	932.4	q_e	884.12
	k_2	0.0121	k_2	0.009	k_2	NA

The linear regression values for all of these pseudo-second order data matches are above 94%. Due to the quick rate of adsorption and the tiny scale of the modeled y-

intercepts compared to the high adsorption capacities, the reaction constants k_2 are not very relevant. The equilibrium adsorption capacity q_e is the important factor here and they are very high. In other papers, only a few adsorbents have shown values of adsorption that are this high. An ab initio study on graphene-like materials had a theoretical adsorption capacity of 1280 mg/g lead adsorption [37]. Mesoporous aluminum magnesium oxide composites showed adsorption numbers for arsenic (III) ions at around 813 mg/g [38]. Thiol-functionalized magnesium phyllosilicate clay shows cadmium and lead adsorption capacities at 380 mg/g [39]. These high adsorption numbers from research paper are very rare, traditional adsorption compounds mentioned before such as activated carbons and nanotubes only have adsorption capacities around 100 mg/g [6]. Even compared to these high adsorption capacities from research papers, our hydrogel's capacities are still fairly high.

The cesium adsorption kinetic tests were done using recipe #2. The adsorption curve is shown in Figure 14.

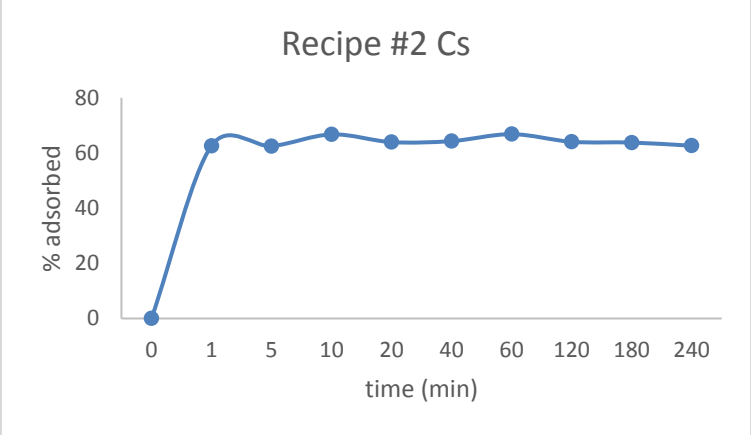

Figure 14. Cesium kinetics adsorption results

These data sets also fit very well with pseudo second order kinetics and the model parameters are shown in Table 11.

Table 11. Pseudo-second order kinetic results for cesium adsorption

Pseudo Second order model		
Recipe #2		
Cs	q_e	179.3
	k_2	NA

This equilibrium capacity is quite high compared to some of the other cesium adsorption compounds. Ferrocyanide functionalized mesoporous silica has adsorption capacity around 30 mg/g [35]. While on the high end of adsorption, resin immobilized copper ferrocyanide showed adsorption capacities of up to 171 mg/g in batch environments [40]. Biomass from marine algae modified with ferrocyanide showed adsorption capacities for cesium at 198.7 mg/g [36]. All three of these compounds from other research showed equilibrium times around 20 minutes, which is significantly slower than our equilibrium time of less than 5 minutes. This difference in uptake speed will give our hydrogels an advantage in high speed steady state environments.

4.5 pH tests

The pH of a medium is an important factor which could have a large effect on the adsorption of our hydrogels. In these pH tests, we tried to keep the range within 2-8 to

better match the tradition pH values of production and industrial wastewaters. The adsorption results are summarized in the graphs in Figure 15.

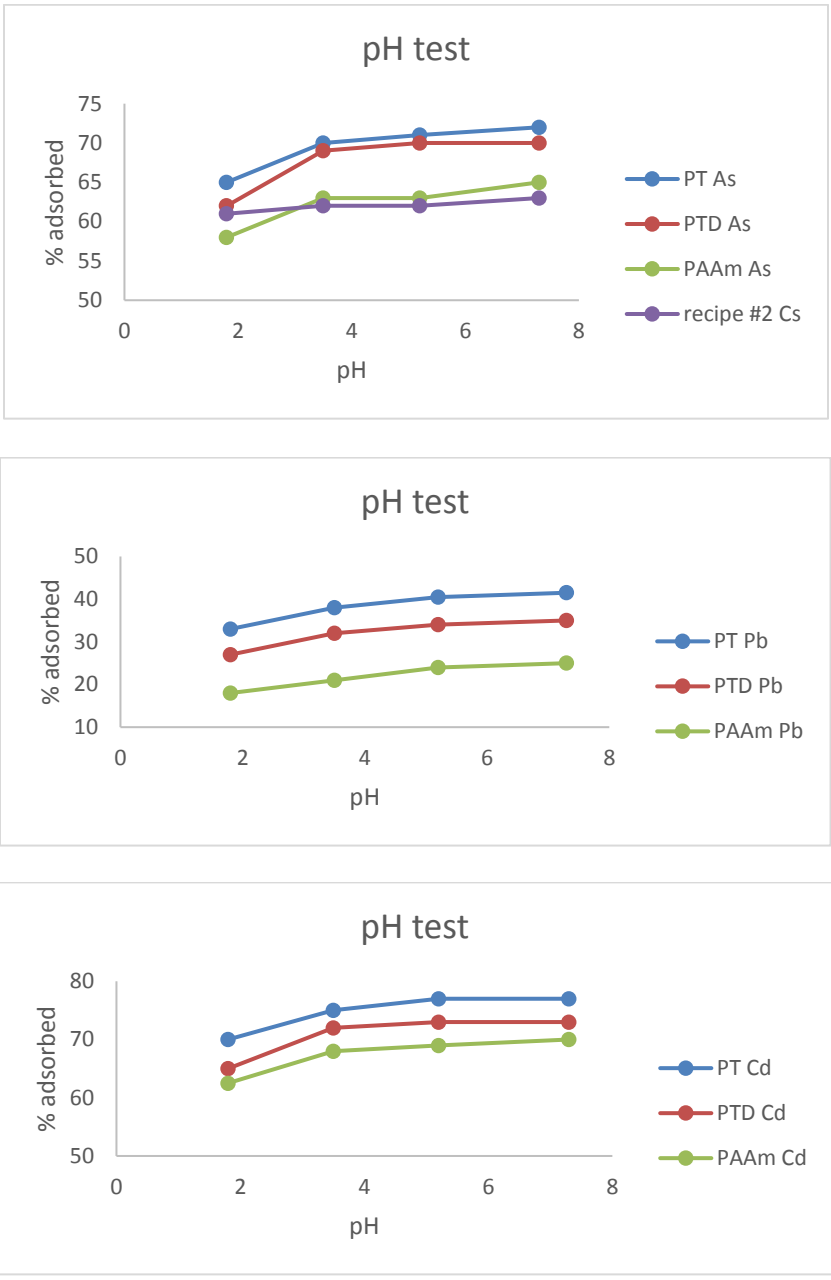

Figure 15. pH adsorption test results

The adsorption profiles as a function of pH for all heavy metal hydrogels are all very similar in shape. The profiles show that the adsorption is not significantly affected by pH around the ranges of 3.5 – 7.5. But when the pH is more acidic than that, a definite decrease for adsorption can be seen. This was assumed to be the result of high concentrations of hydrogen protons in the solution which naturally bond with ligand groups and hinder heavy metal bonding. This result helped explain why adsorption capacities in this study were higher than those in Dr. Mohammadi's dissertation.

In the case of cesium hydrogels, this change in adsorption due to low pH is minor. Since the reaction between the modified hydrogel and cesium is not the result of metal chelation bonding, but rather a combination of physical adsorption and water coordination, the change in pH will have little effect on the process. This behavior matches the data shown from the biomass ferrocyanide research [36].

4.6 Reusability tests

For these hydrogels to be considered useful in a practical sense, reusability must be considered. By washing the hydrogels with acid after adsorption and using them to re-adsorb more contaminants, we were able to quantify how well and how many times they can be reused. For heavy metal hydrogels, the experimental data showed that adsorbed metals were sufficiently eluted from the gel 5 different times. Below in Figure 16 are the reusability test results for base PAAm and the 2 modified hydrogels for heavy metals.

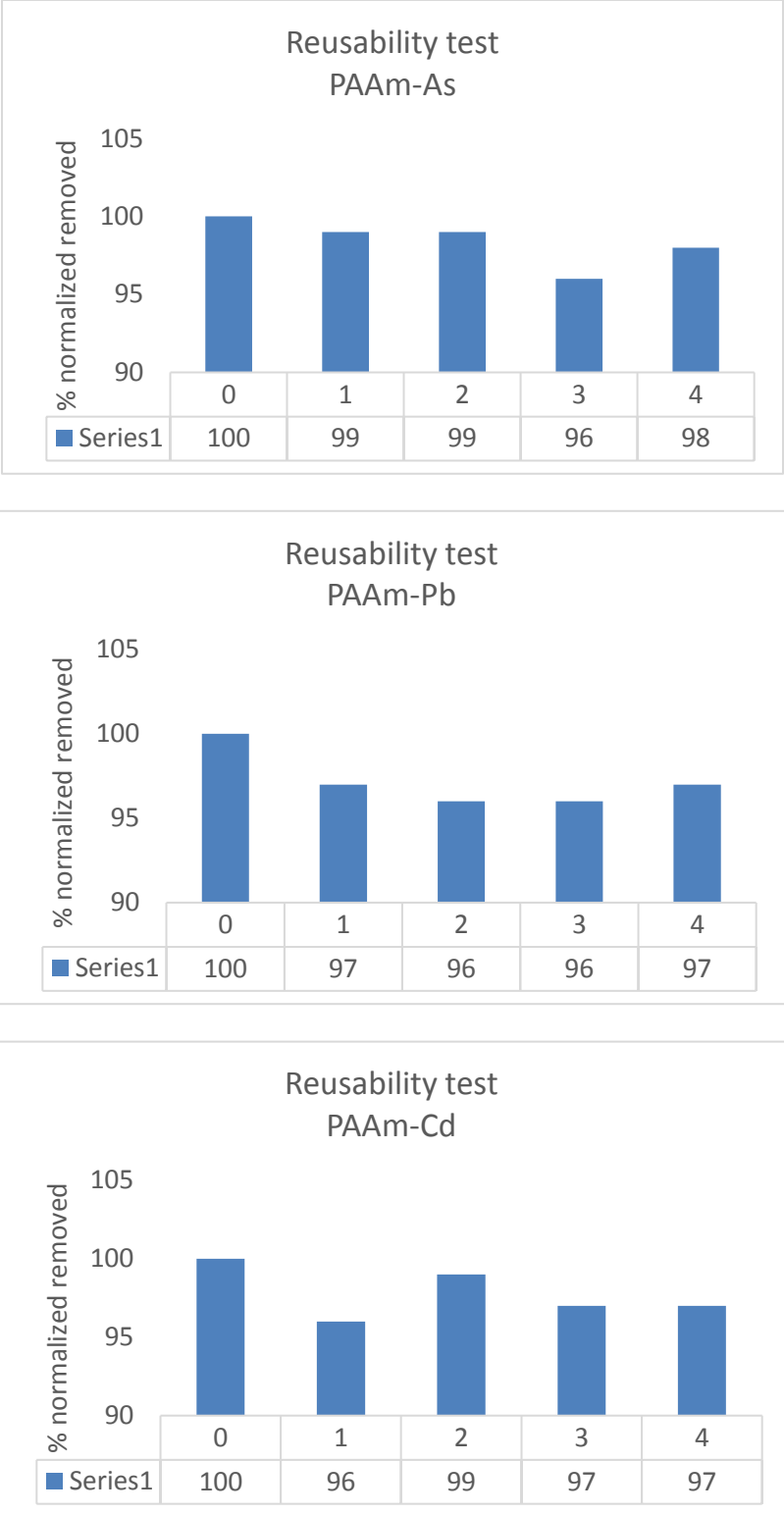

Figure 16. All heavy metal reusability test results

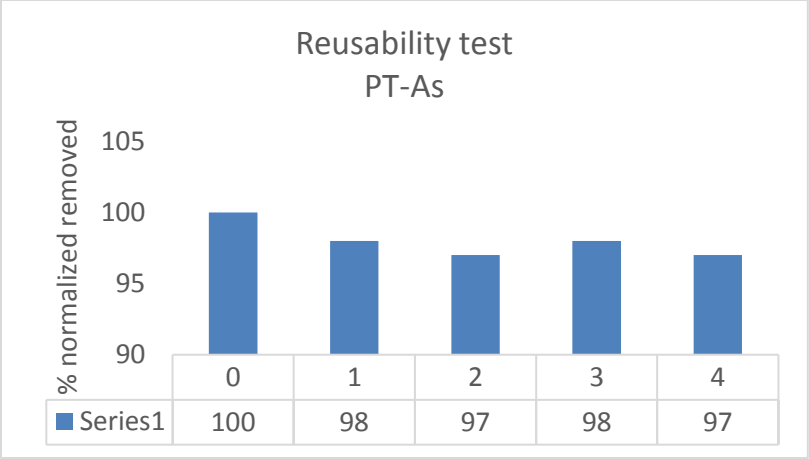

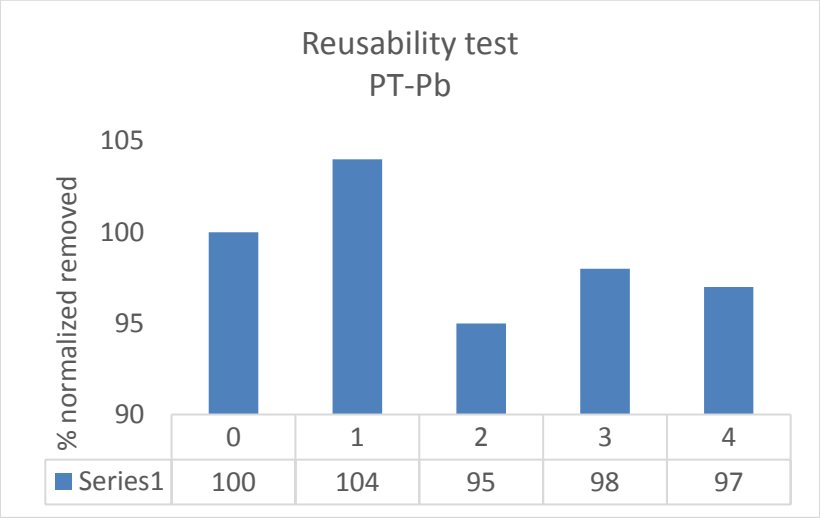

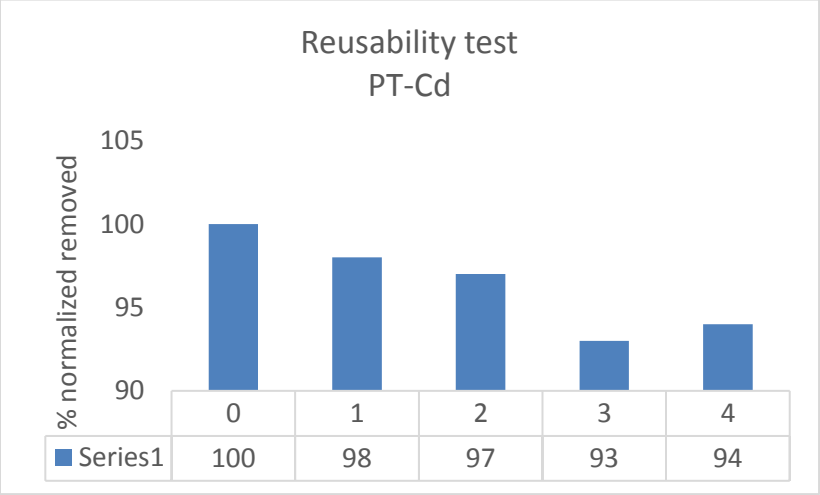

Figure 16. Continued

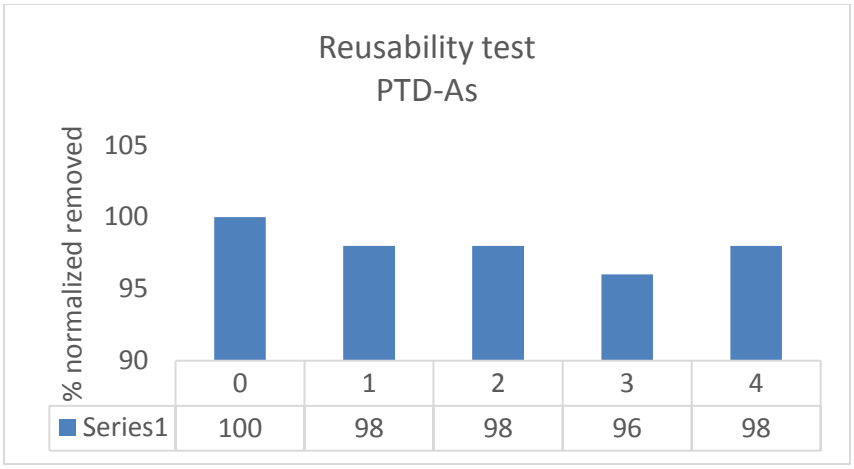

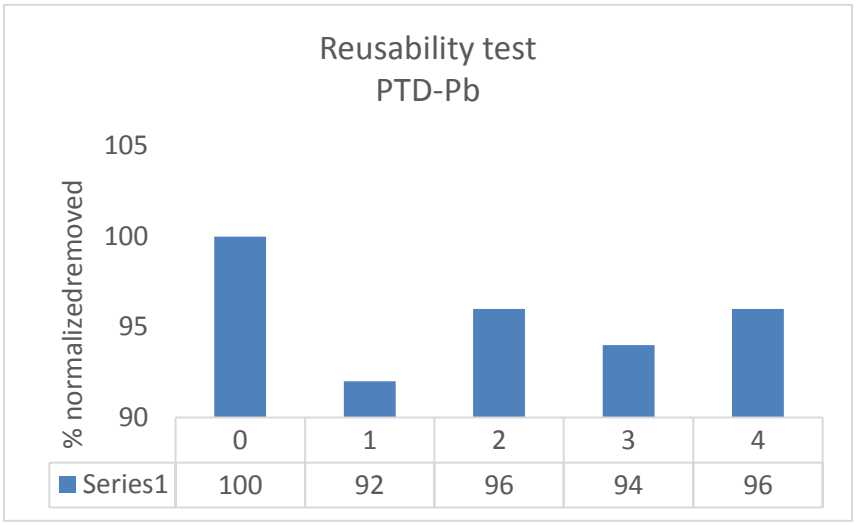

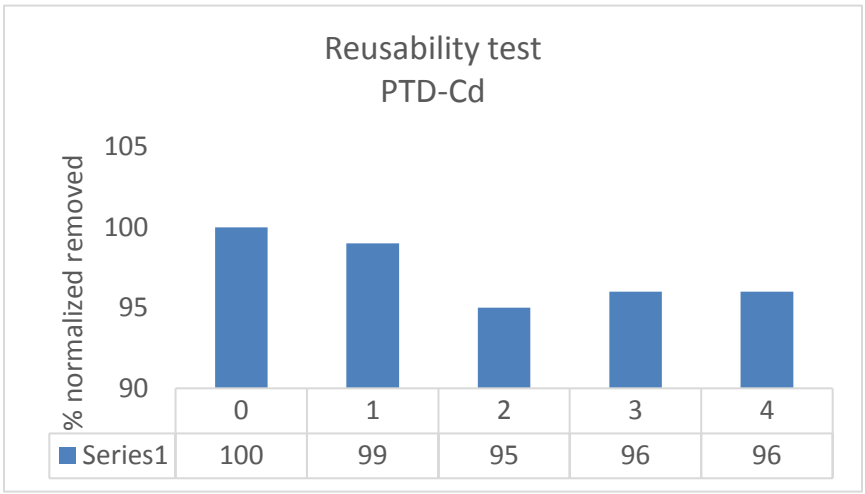

Figure 16. Continued

As we can see, all of the heavy metal hydrogels reacted very well to the HCl treatment and were able to perform almost like new even after 5 cycles. The reasons for this reusability is due partially to our hydrogel being naturally pH sensitive and being able to swell in low pH environments to release ions, and partially to the increased concentrations of hydrogen which compete with heavy metal binding sites. From literature, the thiol modified clays that had high capacities for cadmium and lead showed 98% desorption of heavy metals after the initial adsorption and good reusability [39]. The mesoporous aluminum magnesium oxide composites that had high arsenic adsorption, showed unsatisfactory desorption and reusability [38].

Since the capture of cesium is not due to the coordination bonding of ligands and metals, but rather by physical adsorption and hydrophilic action, the acid treatment did not do much for its reusability. Cesium reusability results are shown below in Figure 17.

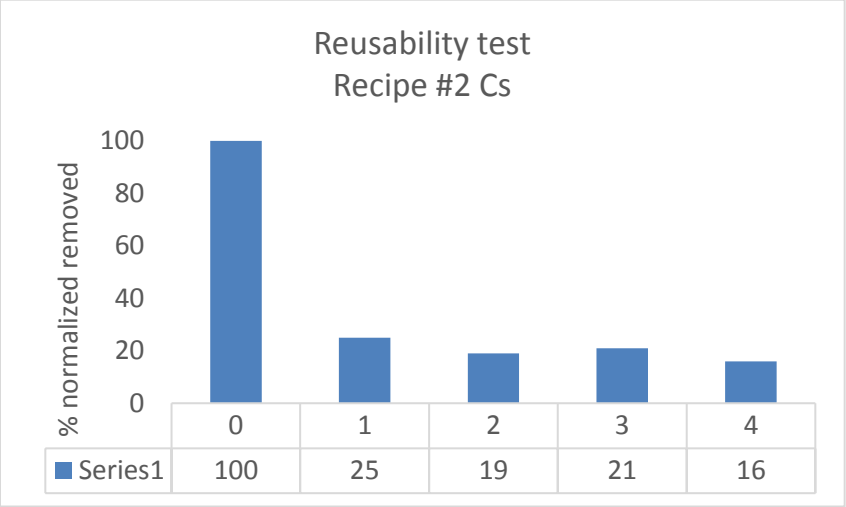

Figure 17. Cesium reusability results

The first adsorption experiment after its initial adsorption and acid wash was only able to adsorb 25% of its original capacity, while subsequent times showed even lower numbers. The reason that these adsorption numbers are not zero after the first time is most likely because of non-occupied capture sites from the first run and general adsorption from attraction due to wan der Waals forces. This lack of desorption from washing with acids is also documented in the biomass ferrocyanide paper in which several different acids were used to attempt to desorb cesium [36]. In the paper, all acid washes for desorption failed. Only by washing with 1M KOH and/or NaOH was there desorption of cesium. Even with high desorption percentages, their reusability saw diminishing returns, and their adsorption capacity decreased 10% to 15% each cycle. I believe the usage of KOH and NaOH for reusability testing on our cesium hydrogels should be done in the future.

4.7 Column study

For the last experiment, we wanted to see how well the hydrogels can adsorb contaminants while in a steady state environment. To do this, a rudimentary column study was set up to test how high the capacities of the hydrogels are in flowing fluids. Since PAAm/TGA had outperformed PAAm/TGA/DHBA in all previous experiments, we decided to exclude PAAm/TGA/DHBA in the column study tests. The experiments were done by pumping known amounts of contaminant solution through a thin layer of adsorbent followed by extensive water flushes. These water flushes ended up mixing with the contaminant solution. Although normal column studies have a C_e/C_o y-axis

when plotted, that would not make sense here due to the mixing of water and contaminant solution. Instead I decided to show the graphic results with effluent concentration in the y-axis, which is still useful in showing adsorption. The graphs below in Figure 18 show the concentrations of the fluid collected as a function of 5 ml vials.

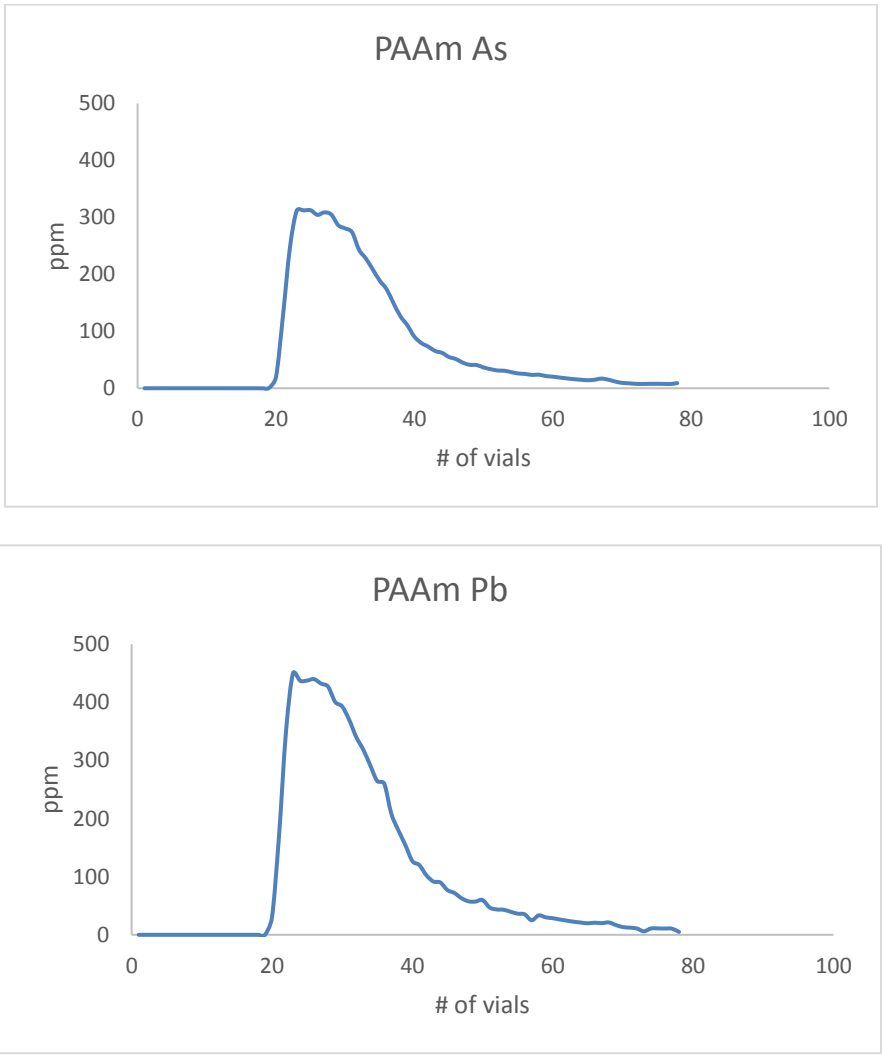

Figure 18. Column study effluent curves

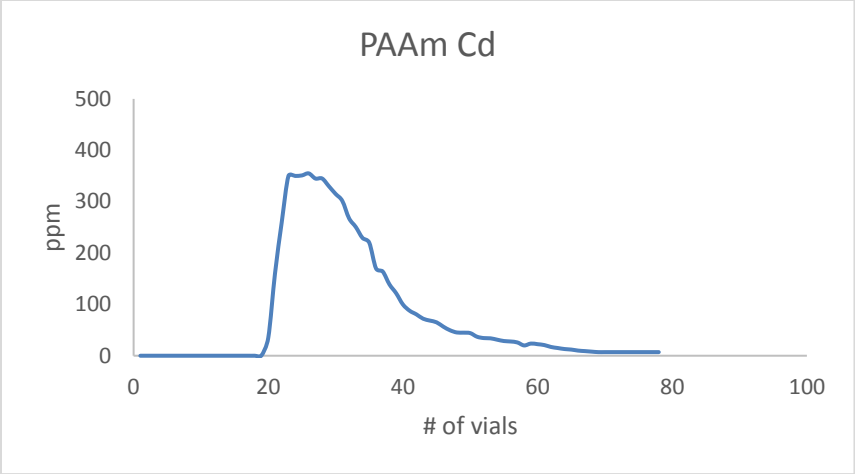

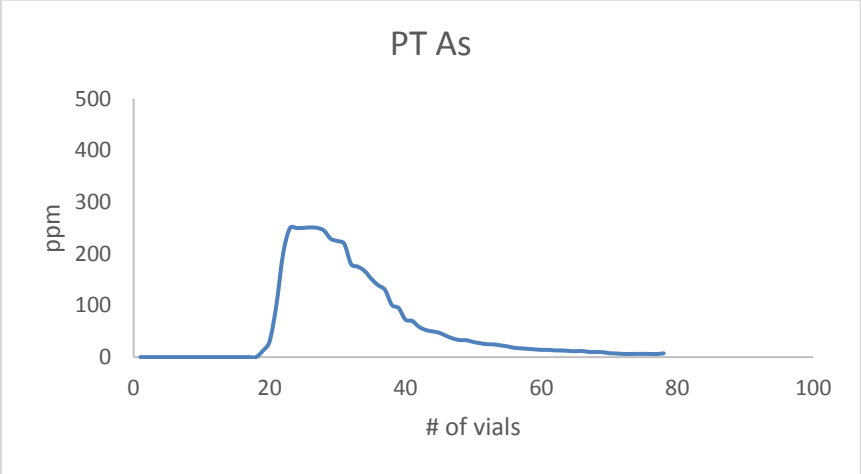

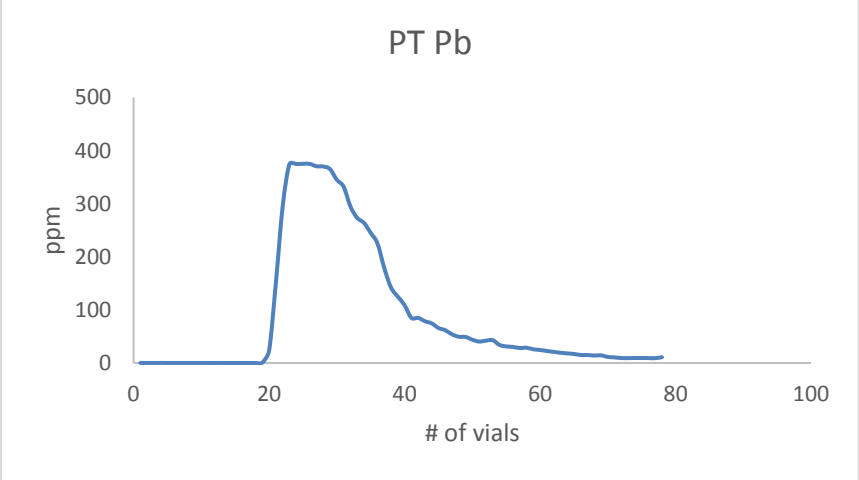

Figure 18. Continued

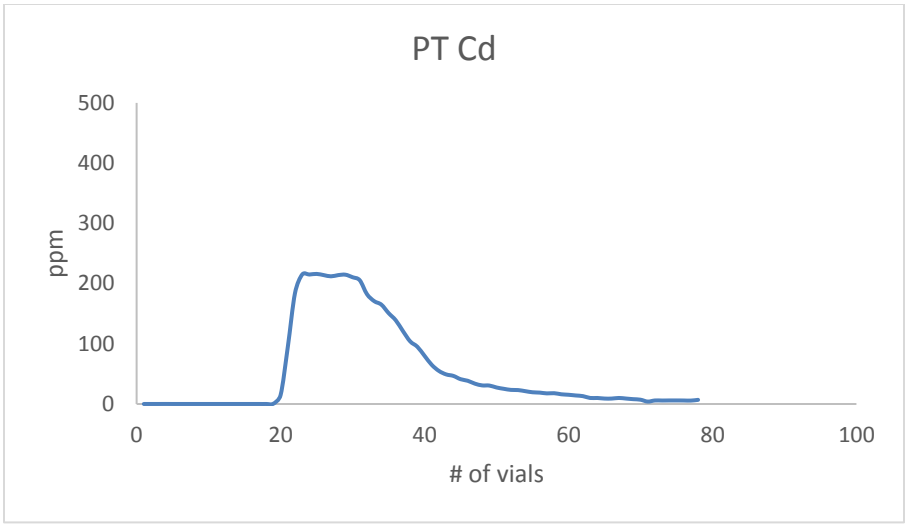

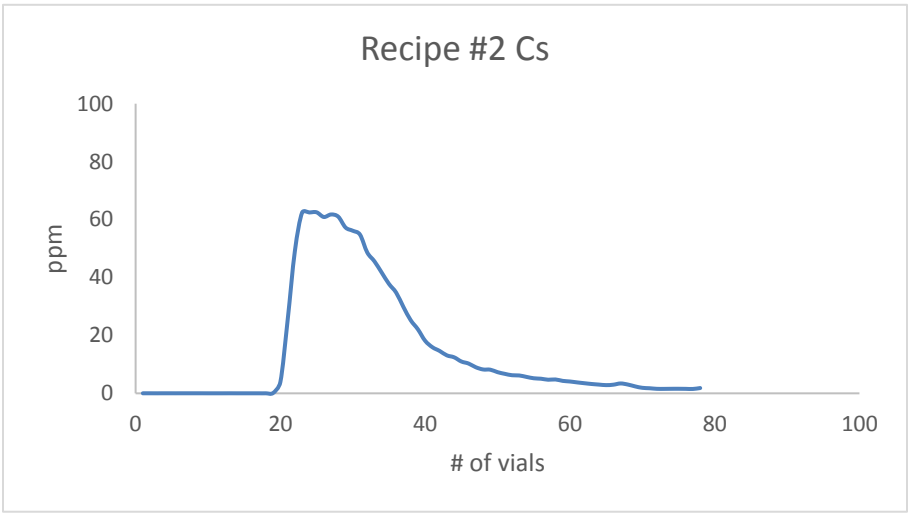

Figure 18. Continued

The shape of the curves shows 4 zones of fluid for each column study. The first zone are the vials of water being pushed out by the contaminant solution which have a 0 ppm reading. In the case of the recipe #2 column study, these are vials 0 to 20. The second zone begins as the concentration of the effluent solutions jump to a high point and remain fairly constant, these are vials 22 to 28 for recipe #2. This zone usually lasts

about 5-10 vials, signaling the base solution being pushed through the column. The third zone shows a fairly quick decrease in effluent concentration, this is most likely due to the bulk of the original solution being pushed through, and thus the remaining solution has lower concentration from mixing with the flush water. These are vials 29 to 40 for recipe #2. The last zone with the lowest concentration show the remaining contaminants being pushed through and most likely certain amounts of desorption from the moving current. Table 12 contains the calculated adsorption capacities for the hydrogels in the column:

Table 12. Column study adsorption capacities

PAAm (mg/g)		PT (mg/g)		Recipe # 2 (mg/g)	
As	528.3	As	717.4	Cs	109.57
Pb	314.95	Pb	373.28		
Cd	507.85	Cd	708.78		

As can be seen in these adsorption capacities, the hydrogels perform with lower capacities compared to the batch environment. Since the kinetics experiments showed extremely fast adsorption, it is understandable that these adsorption capacities are still fairly high. The reduction in capacity can be explained partially due to the column procedures and effects of the flushing water. Because the column study was done by injection of a limited amount of contaminant solution followed by a water flush, there was most likely dilution between the two. When the solution was diluted, the adsorption

capacity, being a function of concentration, will then reflect the lower adsorption capacities. In this case, contaminant solutions were most likely diluted in zones 3 and 4 to concentrations much lower than the original, thus resulting in lower equilibrium capacities. The second reason for this decreased capacity was pointed out in a paper on adsorption of pesticides in soils [32]. In a column study with pesticides, Rao et al. pumped standard concentration solutions into his column until the effluent reached a plateau. From there, he pumped a surge of water at the same velocity as his solution to detect how much desorption and non-adsorbed solutes he had. In his paper, he was able to retrieve significant amounts of originally perceived adsorbed materials. I believe that due to velocity of the solution and water in my column study, much of the non-adsorbed and weakly adsorbed contaminants are flushed out. A future work experiment to test desorption could be to saturate an amount of hydrogel in a batch setting with the target contaminant, then load it up into a column and push DI water through it. It is unfortunate that all of the papers researching the high adsorption capacity compounds we examined did not perform column studies. Because of this, we do not have similar previous cases to compare our results. Although it can be hypothesized that due to the extremely rapid rate of adsorption for our hydrogels, our column studies should have higher relative adsorption capacities than the other compounds from literature.

5. CONCLUSIONS

Through extensive testing, these hydrogels with functional groups were analyzed to see how well they could adsorb heavy metals and cesium in wastewaters. These experiments provided useful insights on what environments these hydrogels can be used in and how well they would function in such environments. The heavy metal hydrogel PAAm/TGA has shown that it excels in adsorption capacity and speed when tested with cadmium, lead, and arsenic ions. The cesium adsorption hydrogel also showed extremely fast uptake and relatively high adsorption numbers. We were able to learn that heavy metal adsorption hydrogels will function well in solutions with iron, copper, and zinc contaminants, and that it should be used in wastewaters with pH above 4. The cesium adsorption hydrogels showed no significant decrease in functionality even in low pH environments, which was similar to results in the biomass ferrocyanide paper [36]. Even in a steady state setting, the adsorption capacity of both heavy metal and cesium adsorption hydrogels are still greater than some of its competitors. Although the base PAAm hydrogel with no functional groups showed great adsorption of heavy metals, it is evident that the addition of TGA has helped in the adsorption process. The heavy metal hydrogels had outstanding results in recoverability and showed above 90% recovery even after 5 cycles. It was unfortunate that the cesium adsorption hydrogels were not able to be successfully recovered like the heavy metal hydrogels through acid wash.

Due to its fast and high adsorption capacity, I do recommend further studies be done on the cesium hydrogels, especially with KOH and NaOH as potential desorption solutions. Even though biomass algae functionalized with ferrocyanide outperforms the cesium hydrogels from this study, they can still be useful. The heavy metal adsorption hydrogels showed great promise, and future testing, especially on desorption, would be a good idea. In the end, I believe that further testing in a more traditional steady state column study, with a constant injection of large amounts of contaminant solutions, on PAAm, PAAm/TGA, and cesium capturing hydrogels could better enlighten us on how well they would perform in a large scale steady state environment.

REFERENCES

1. Azetsu-Scott, K., Yeats, P., Wohlgeschaffen, G., Dalziel, J., Niven, S. et al (2007). Precipitation of heavy metals in produced water: Influence on contaminant transport and toxicity. Marine environmental research, 63(2), 146-167.

2. Guo, X., Du, B., Wei, Q., Yang, J., Hu, L. et al. (2014). Synthesis of amino functionalized magnetic graphenes composite material and its application to remove Cr (VI), Pb (II), Hg (II), Cd (II) and Ni (II) from contaminated water. Journal of hazardous materials, 278, 211-220.

3. Kieu, H. T., Müller, E., & Horn, H. (2011). Heavy metal removal in anaerobic semi-continuous stirred tank reactors by a consortium of sulfate-reducing bacteria. Water research, 45(13), 3863-3870.

4. Liu, X., Chen, G. R., Lee, D. J., Kawamoto, T., Tanaka, H. et al. (2014). Adsorption removal of cesium from drinking waters: A mini review on use of biosorbents and other adsorbents. Bioresource technology, 160, 142-149.

5. Tokuyama, H., Yoshida, T., & He, L. (2011). Preparation of novel emulsion gel adsorbents and their adsorption properties for heavy-metal ions. Industrial & Engineering Chemistry Research, 50(17), 10270-10277.

6. Fu, F., & Wang, Q. (2011). Removal of heavy metal ions from wastewaters: a review. Journal of environmental management, 92(3), 407-418.

7. Hamasaki, T., Nakamichi, N., Teruya, K., & Shirahata, S. (2014). Removal efficiency of radioactive cesium and iodine ions by a flow-type apparatus designed for electrochemically reduced water production. PloS one, 9(7), e102218.

8. Mohammadi, Z., Xie, S. X., Golub, A. L., Gehrke, S. H., & Berkland, C. (2011). Siderophore-Mimetic hydrogel for iron chelation therapy. Journal of Applied Polymer Science, 121(3), 1384-1392.

9. Flora, S. J., & Pachauri, V. (2010). Chelation in metal intoxication. International journal of environmental research and public health, 7(7), 2745-2788.

10. Chen, G. R., Chang, Y. R., Liu, X., Kawamoto, T., Tanaka, H. et al. (2015). Prussian blue (PB) granules for cesium (Cs) removal from drinking water. Separation and Purification Technology, 143, 146-151.

11. Ten chemicals of major public health concern. (n.d.). Retrieved July 29, 2016, from http://www.who.int/ipcs/assessment/public_health/chemicals_phc/en/

12. Järup, L. (2003). Hazards of heavy metal contamination. British medical bulletin, 68(1), 167-182.

13. Steinhauser, G., Brandl, A., & Johnson, T. E. (2014). Comparison of the Chernobyl and Fukushima nuclear accidents: A review of the environmental impacts. Science of the Total Environment, 470, 800-817.

14. Lipscy, P. Y., Kushida, K. E., & Incerti, T. (2013). The Fukushima disaster and Japan's nuclear plant vulnerability in comparative perspective. Environmental science & technology, 47(12), 6082-6088.

15. Finch, S. C. (1987). Acute radiation syndrome. JAMA, 258(5), 664-667.

16. Christodouleas, J. P., Forrest, R. D., Ainsley, C. G., Tochner, Z., Hahn, S. M. et al. (2011). Short-term and long-term health risks of nuclear-power-plant accidents. New England journal of medicine, 364(24), 2334-2341.

17. Nurchi, V. M., & Villaescusa, I. (2012). Sorption of toxic metal ions by solid sorbents: a predictive speciation approach based on complex formation constants in aqueous solution. Coordination Chemistry Reviews, 256(1), 212-221.

18. Andersen, O. (1999). Principles and recent developments in chelation treatment of metal intoxication. Chemical reviews, 99(9), 2683-2710.

19. Raymond, K. N., Dertz, E. A., & Kim, S. S. (2003). Enterobactin: an archetype for microbial iron transport. Proceedings of the National Academy of Sciences, 100(7), 3584-3588.

20. Mohammadi, Z. (2011). Metal-binding polymers as chelating agents (Doctoral dissertation, University of Kansas).

21. George, S., Benny, P. J., Sunny, K., & Cincy, G. (2011). Antibiotic activity of 2, 3-dihydroxybenzoic acid isolated from Flacourtia inermis fruit against multi drug resistant bacteria. Asian J Pharm Clin Res, 4, 126-130.

22. Chen, G. R., Chang, Y. R., Liu, X., Kawamoto, T., Tanaka, H. et al. (2015). Prussian blue non-woven filter for cesium removal from drinking water. Separation and Purification Technology, 153, 37-42.

23. Ishizaki, M., Akiba, S., Ohtani, A., Hoshi, Y., Ono, K. et al. (2013). Proton-exchange mechanism of specific Cs+ adsorption via lattice defect sites of

Prussian blue filled with coordination and crystallization water molecules. Dalton Transactions, 42(45), 16049-16055.

24. Qiu, H., Lv, L., Pan, B. C., Zhang, Q. J., Zhang et al. (2009). Critical review in adsorption kinetic models. Journal of Zhejiang University Science A, 10(5), 716-724.

25. Ho, Y. S., & McKay, G. (1999). Pseudo-second order model for sorption processes. Process biochemistry, 34(5), 451-465.

26. Ho, Y. S., & McKay, G. (2000). The kinetics of sorption of divalent metal ions onto sphagnum moss peat. Water research, 34(3), 735-742.

27. Dada, A. O., Olalekan, A. P., Olatunya, A. M., & Dada, O. (2012). Langmuir, Freundlich, Temkin and Dubinin–Radushkevich isotherms studies of equilibrium sorption of Zn2+ unto phosphoric acid modified rice husk. Journal of Applied Chemistry, 3(1), 38-45.

28. Volesky, B., & Holan, Z. R. (1995). Biosorption of heavy metals. Biotechnology progress, 11(3), 235-250.

29. Hameed, B. H., Salman, J. M., & Ahmad, A. L. (2009). Adsorption isotherm and kinetic modeling of 2, 4-D pesticide on activated carbon derived from date stones. Journal of Hazardous Materials, 163(1), 121-126.

30. Amuda, O. S., Giwa, A., & Bello, I. A. (2007). Removal of heavy metal from industrial wastewater using modified activated coconut shell carbon. Biochemical Engineering Journal, 36(2), 174-181.

31. Stafiej, A., & Pyrzynska, K. (2007). Adsorption of heavy metal ions with carbon nanotubes. Separation and Purification Technology, 58(1), 49-52.

32. Rao, P. S. C., & Davidson, J. M. (1979). Adsorption and movement of selected pesticides at high concentrations in soils. Water Research, 13(4), 375-380.

33. Park, J. H., Cho, J. S., Ok, Y. S., Kim, S. H., Kang, S. W. et al. (2015). Competitive adsorption and selectivity sequence of heavy metals by chicken bone-derived biochar: Batch and column experiment. Journal of Environmental Science and Health, Part A, 50(11), 1194-1204.

34. Yong, R. N., & Phadungchewit, Y. (1993). pH influence on selectivity and retention of heavy metals in some clay soils. Canadian Geotechnical Journal, 30(5), 821-833.

35. Sangvanich, T., Sukwarotwat, V., Wiacek, R. J., Grudzien, R. M., Fryxell, G. E. et al. (2010). Selective capture of cesium and thallium from natural waters and simulated wastes with copper ferrocyanide functionalized mesoporous silica. Journal of hazardous materials, 182(1), 225-231.

36. Jalali-Rad, R., Ghafourian, H., Asef, Y., Dalir, S. T., Sahafipour, M. H. et al. (2004). Biosorption of cesium by native and chemically modified biomass of marine algae: introduce the new biosorbents for biotechnology applications. Journal of hazardous materials, 116(1), 125-134.

37. Guo, X., Zhang, X., Zhao, S., Huang, Q., & Xue, J. (2016). High adsorption capacity of heavy metals on two-dimensional MXenes: an ab initio study with molecular dynamics simulation. Physical Chemistry Chemical Physics, 18(1), 228-233.

38. Li, W., Chen, D., Xia, F., Tan, J. Z., Huang, P. P. et al. (2016). Extremely high arsenic removal capacity for mesoporous aluminium magnesium oxide composites. Environmental Science: Nano, 3(1), 94-106.

39. Lagadic, I. L., Mitchell, M. K., & Payne, B. D. (2001). Highly effective adsorption of heavy metal ions by a thiol-functionalized magnesium phyllosilicate clay. Environmental science & technology, 35(5), 984-990.

40. Clarke, T. D., & Wai, C. M. (1998). Selective removal of cesium from acid solutions with immobilized copper ferrocyanide. Analytical chemistry, 70(17), 3708-3711.

APPENDIX

This appendix section will show sample calculations using the kinetic and isotherm modeling explained in section 2.5 of this thesis.

A.1 Pseudo first order kinetic modeling

Use the following linearized kinetic equation and data to perform sample calculations for pseudo first order Lagergren kinetic modeling.

$$\log(q_e - q_t) = log q_e + \frac{k_1}{2.303} t \qquad (11)$$

Time (min)	Normalized adsorption (mg/g)
0	0
1	281.64
5	231.45
10	273.31
20	365.56
40	313.24
60	356.32
120	449.28
180	420.39
240	433.72

From this data, we are able to extract values for time (t), adsorption capacities at time (q_t), and adsorption capacity at equilibrium (q_e), which we assume is 433.72 mg/g. Using these points, plot a graph of $\log(q_e - q_t)$ vs.t and calculate the slope and y-intercept.

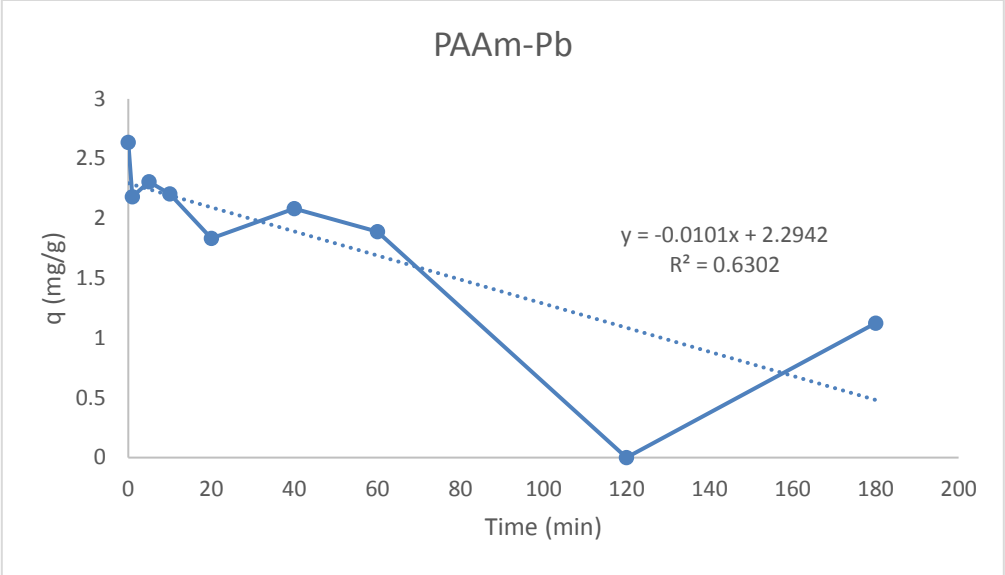

We can use slope from the trend line to fit the Lagergren equation slope $\frac{k_1}{2.303} = -0.0101$ to calculate k_1. Multiply the slope by 2.303 to solve for k_1 as -0.0233.

A.2 Pseudo second order kinetic modeling

Use the following linearized kinetic equation and data to perform sample calculations for pseudo second order Ho kinetic modeling.

$$\frac{t}{q_t} = \frac{1}{k_2 q_e^2} + \frac{t}{q_e} \qquad (12)$$

Time (min)	Normalized adsorption (mg/g)
0	0
1	281.64
5	231.45
10	273.31
20	365.56
40	313.24

60	356.32
120	449.28
180	420.39
240	433.72

From this data, we are able to extract values for time (t), adsorption capacities at time (q_t). This time we will leave the adsorption capacity at equilibrium (q_e) as a variable to be calculated. Plot a graph with t/qt vs. t so we can calculate the slope and intercept and solve for k2 and qe.

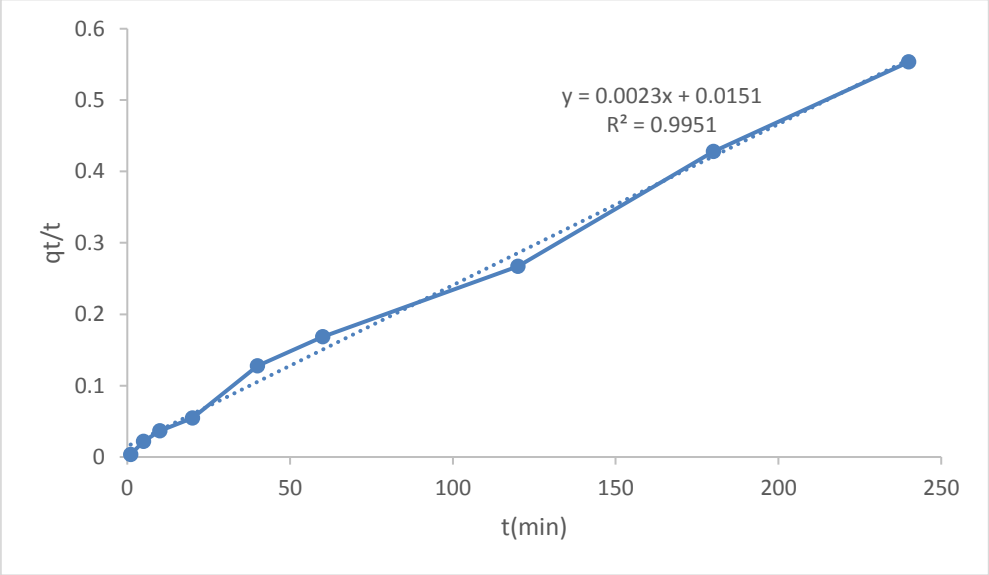

From the trend line we can fit the slope to the Ho equation $0.0023 = \frac{1}{q_e}$ and inverse it to get the value of q_e as 434.78 mg/g. Next, plug the new q_e value into the formula for the intercept $0.0151 = \frac{1}{k_2 q_e^2}$ to calculate k_2 as 0.00035.

A.3 Langmuir isotherm modeling

Use the following linearized isotherm equation and data to perform sample calculations for Langmuir isotherm modeling.

$$\frac{1}{q_e} = \frac{1}{q_{max}} + \frac{1}{q_{max} K_L C_e} \quad (13)$$

qe	ce
Absorbed/gel (mg/g)	conc. (mg/mL)
5	0.0025
31.52	0.00424
82.87	0.008565
170.6	0.0147
333.32	0.03334
669.77	0.065115
869.7	0.06515

From this data, we are able to extract values for equilibrium concentration of adsorbate (c_e) and adsorption capacity at equilibrium (q_e). Plot a graph of $1/q_e$ vs. $1/c_e$ so we can calculate the slope and intercept and solve for K_L and q_{max}.

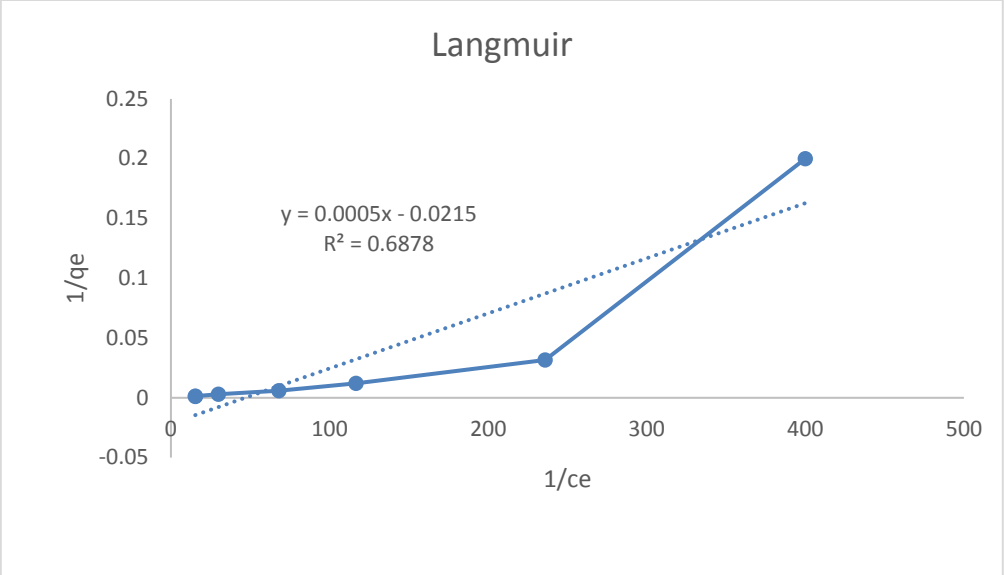

From the trend line we can fit the y-intercept into the formula $\frac{1}{q_{max}} = -0.0215$. Inverse it to get the value of q_{max} as -46.51 mg/g. Next, plug the new q_{max} value into the equation for the slope $0.0005 = \frac{1}{K_L q_{max}}$ to calculate K_L as -43.

A.4 Freundlich isotherm modeling

Use the following linearized isotherm equation and data to perform sample calculations for Freundlich isotherm modeling.

$$logQ_e = logK_f + \frac{1}{n} logC_e \quad (14)$$

qe	ce
Absorbed/gel (mg/g)	conc. (mg/mL)
5	0.0025
31.52	0.00424
82.87	0.008565

170.6	0.0147
333.32	0.03334
669.77	0.065115
869.7	0.06515

From this data, we are able to extract values for equilibrium concentration of adsorbate (c_e) and adsorption capacity at equilibrium (q_e). Plot a graph of $LogQ_e$ vs. $LogC_e$ so we can calculate the slope and intercept and solve for K_f and n.

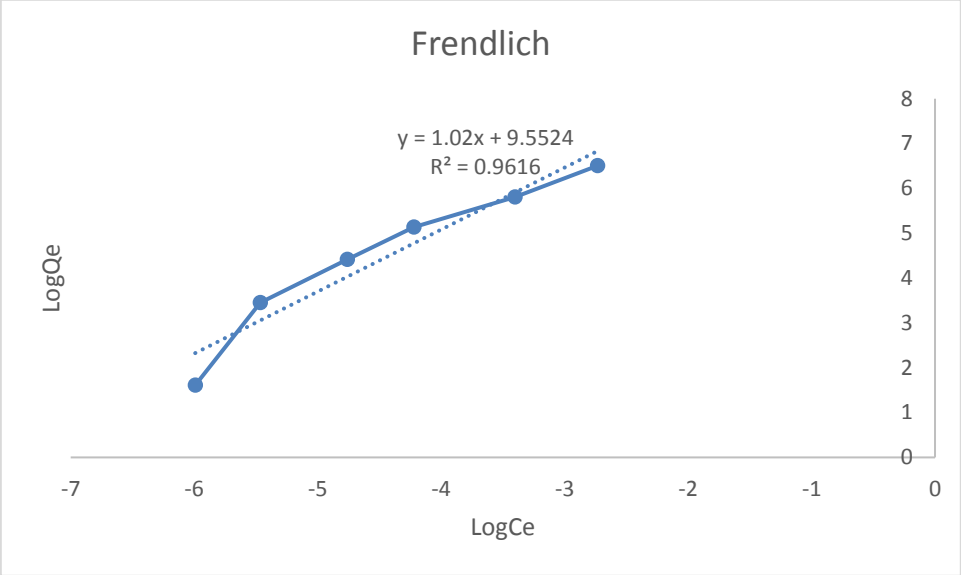

From the trend line we can fit the y-intercept $LogK_f = 9.5524$ in this plot. Inverse Log that intercept to receive the value of K_f as 14078.44. Next, use the equation for the slope $1.02 = \frac{1}{n}$ to calculate n as 0.98.

A.5 Temkin isotherm modeling

Use the following linearized isotherm equation and data to perform sample calculations for Temkin isotherm modeling.

$$q_e = \frac{RT}{b}\ln(A_T) + \frac{RT}{b}\ln(C_e) \quad (15)$$

qe	ce
Absorbed/gel (mg/g)	conc. (mg/mL)
5	0.0025
31.52	0.00424
82.87	0.008565
170.6	0.0147
333.32	0.03334
669.77	0.065115
869.7	0.06515

From this data, we are able to extract values for equilibrium concentration of adsorbate (c_e) and adsorption capacity at equilibrium (q_e). Plot a line with q_e vs. Ln(C_e) so we can calculate the slope and intercept and solve for RT/b and A_T.

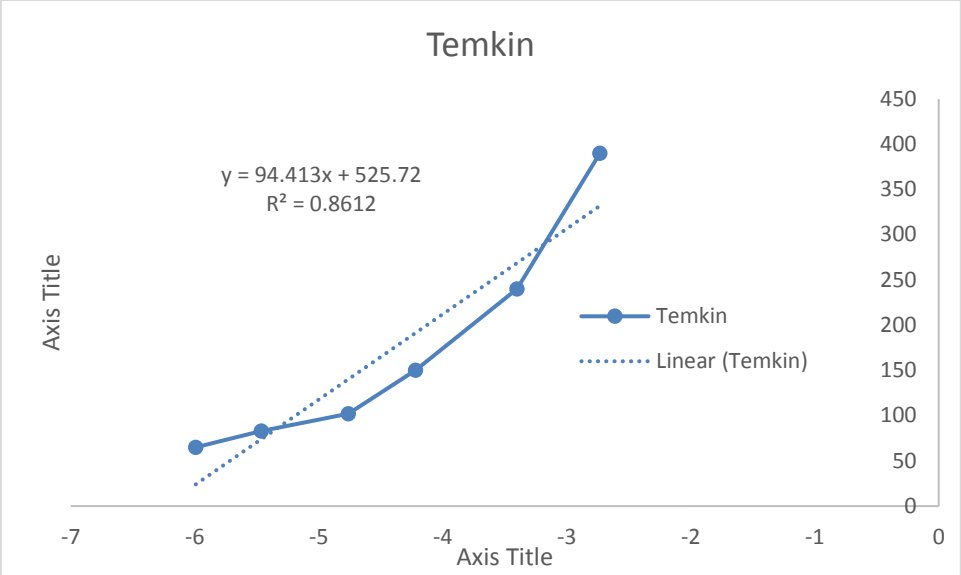

From the trend line we can fit the slope to $\frac{RT}{b} = 94.413$ in this plot. Use the value of 94.413 as the slope and input it into $525.72 = \frac{RT}{b}\ln(A_T)$ to calculate A_T as 261.7.